An experimental study into the dynamics of vortex rings

ES327 3rd Year Project (MEng)

JOSEPH MURPHY

SUMMARY

The aim of this project was to study the dynamics of vortex rings. This involved the adaptation of previous student's projects, specifically designing an ink injection system for clearer visualisation of the vortex rings. Once the system was optimised for clear vortex ring production, various measurements and observations were made for the vortex rings produced at a range of parameters.

One of the measurements recorded from the produced rings was the translational velocity. The testing consisted of measuring the displacement of the ring against the time since ejection producing a plot of the translational propagation of the vortex ring. An average of this plot was taken to produce a trend line and therefore provide the gradient, thus providing the average velocity. The independent variable for the production of the vortex rings was the piston speed, ranging from 4.54cm/s (50g) to 27.42cm/s (200g) while the diameter of the nozzle and the stroke length were kept constant. The resulting ring velocities ranged between 1.7cm/s to 7.2cm/s. The measured velocities were compared with data produced from previous experimental research and showed strong similarities. The measured velocities were also compared with theoretically predicted velocities, and although this comparison wasn't as close as the previous experimental research, it did show enough similarity to be considered reasonable.

Another observation of the vortex rings that was recorded was their instability. The visualisation of the instability was varied however for a significant portion of the modes (6-12), an image that was clear enough to interpret was recorded. The parameters that formed these modes of instabilities were compared with previous research and proved promising. Research that specifically focused on the lower modes of the instability (5-13) was compared with the with the experimental data and although other parameters varied, causing some disparity between the data sets, the data which was comparable showed strong similarities. For example, similar Reynolds number producing a the same mode of instability. The distance before the instability transitioned to turbulence was also compared and showed strong similarities.

The portion of the project that had not yet been previously researched, focused on the possibility of imposing an instability on a vortex ring. This was tested by producing a nozzle that had the form of an instability as its aperture. The rings produced from these nozzles varied in clarity in regard to analysing them, however, a conclusion was made upon the clearest recordings. The nozzle produced a vortex ring with the same form as the nozzle, and therefore the same shape as an instability, however this was not actually an instability. This was concluded as although the form is similar, the motion of the fluid is completely different. The ring would initially hold the wavy shape before transitioning back to a circular ring, then forming an instability identical to previous standard results.

CONTENTS

LIST OF FIGURES

NOMENCLATURE

Symbols

U	Translational velocity of vortex ring
Γ	Circulation
D	Diameter of ring
a	Radius of the rings core
ν	Kinematic viscosity
t	Time
D_M	Diameter of nozzle
L	Stroke Length of piston
U_P	Velocity of piston
Z	Translational displacement from nozzle
n	The Mode of the instability/The number of waves in the instability
Re_r	The Reynolds number of the ring
Re_p	The Reynolds number of the piston
μ	Dynamic viscosity

1 INTRODUCTION

1.1 CONTEXT

Whether it be via the complex method of propulsion used by jellyfish (Costello, et al., 2019), the wake of each flap from a hovering hummingbird (Wolf, 2013), or simply the production by a dolphin for its enjoyment (Lundgren & Mansour, 1991) (cf Figure 2), vortex rings frequently occur naturally in all forms of nature. Other examples that are more likely to be recognised include the mushroom shaped aftermath of an explosion (cf. Figure 1) or a smoke ring generated by a smoker. Needless to say, the shear amount of presence vortex rings have in the naturally occurring world has warranted a significant amount of interest into their origins, boundaries and potential capabilities.

Figure 2 – A dolphin playing with a vortex ring (Aitchtuoh, 2015)

Figure 1 – A vortex ring observed in an explosion (Pinheiro, 2014)

Regarding research into vortices, to quote the famous remark of (Kuchemann, 1965), they are often referred to as the "sinews and muscles of fluid motion". For this reason, these fundamental flow structures have intrigued many of the most famous Mathematicians and Physicists.

Vortex rings (cf. Figure 3) and trailing vortices of aeroplanes, under most conditions, undergo a natural sinusoidal instability that amplifies until eventually deforming the vortices to such an extent they become turbulent. This process destroys the structure far more rapidly than viscous or turbulent decay of the individual filaments. (Widnall, 1975).

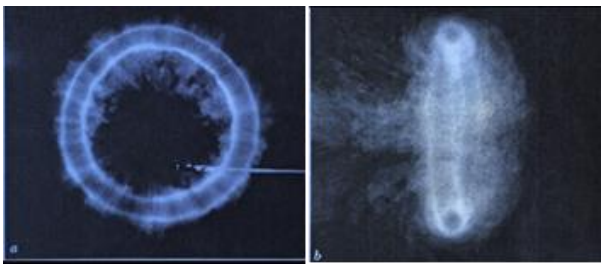

Figure 3 – A vortex ring. (a) Front view; (b) Side view (Akhmetov, 2009)

1.2 AIM

The aim of this project was to investigate the dynamics of vortex rings. The investigation included research on the translational velocity of the rings in addition to observing their instability. A specific focus was placed upon the instability regarding previous research such as the time for the instability to occur, as well as the general form of the instability.

The possibility of altering the naturally occurring instability was also explored. The focus of this experimental research attempted to impose instability modes on vortex rings, during their formation process, that would otherwise not develop naturally. It was planned to impose these modes on the rings through wavy deformations of the generation mechanism. The development of these artificially imposed modes, and of the rings as a whole, were studied by means of flow visualisation techniques.

1.3 OBJECTIVES

- Design and engineer a nozzle that can be easily attached temporarily in addition to providing the necessary mechanisms to facilitate flow visualisation techniques
- Utilise CAD software (Autodesk Fusion 360) to build a 3D model of a circular nozzle capable of attaching to the apparatus as previously engineered – 3D print this structure
- Using the circular shaped nozzle, produce vortex rings observing:
    - The translational velocity of the propagating rings
    - Whether the vortex rings show instabilities comparable to previous research - (Krutzsch, 1939) and (Widnall, 1973) as a control to ensure the next step - experimental testing - is credible.
- Utilise the same CAD model as for the earlier control, however, alter the aperture to take the form of an instability - 3D print
- Attach the new nozzle and attempt to produce vortex rings in the same method as before, observing:
    - The translational velocity of the propagating rings
    - The instability of the vortex rings
- Repeat generation of the vortex rings to ensure a conclusive consistent outcome
- Attempt to analyse the experimental results and propose an explanation.

2 LITERATURE REVIEW

2.1 ORIGINS

Research into the dynamics of vortex rings dates back to, at least, the seminal papers of Hemholtz [1858] and Kelvin [1867]. Hermann von Helmholtz's research paper (Helmholtz, 1858) was one of the most influential papers of its time. Helmholtz developed the fundamental laws of vortex rings within a perfect fluid; in addition to the first mention of vortex lines, vortex filaments and a description/formula of how the vortex ring travels through a medium. This guided the following research of famous names such as (Lord Kelvin) (Thompson, 1867) and (Reynolds, 1876) to developing the understanding of the dynamics of vortex rings.

Helmholtz's theorems – even if only valid for perfect fluids – led Kelvin to the conclusion that these stable, "infinitely strong and infinitely rigid pieces of matter" (Helmhotz's rings) are the basic constituent of matter, as explained in Kelvins paper on the vortex theory of atoms (Thompson, 1867). It is clear now that this was a rash conclusion, however, this did lead to significant research into the dynamics of vortex rings, specifically their stability.

2.2 THE TRANSLATIONAL VELOCITY OF THE VORTEX RING

2.2.1 Theoretical Research

Some of the earliest research into the dynamics of vortex rings was regarding the translational velocity U – the speed at which the ring propagates the length of the tank starting from the nozzle.

Hicks explored the theoretical approach to calculating the translational velocity of vortex rings (Hicks, 1885). For a uniform thin cored vortex ring, the equation for the velocity was shown to be;

$$U = \frac{\Gamma}{4\pi R}\left[\log\frac{8R}{a} - \frac{1}{4}\right] \quad (1)$$

Where Γ is the circulation (see section3.3), R is the radius of the ring and a is the core radius. There has however been controversy on the value of the constant (-1/4) as other researchers have arrived at different results (such as -1 instead) (Saffman, 1995).

Although these formulas were valuable in calculating the maximum velocity comparing different formations, it was noted that as the vortex ring propagates through the tank, the velocity decreases. (Maxworthy, 1972). Maxworthy mentioned that it was originally Reynolds that noted this phenomenon and attributed it to the volume of the vortex ring increasing due to viscous deformation, and that this volume increase induced a velocity decrease in order to conserve

momentum. This was considered by Saffman, by including a Gaussian velocity profile in the vorticity core that would account for the growth in volume due to viscous diffusion (Saffman, 1970). This resulted in his formula for the velocity of a viscous vortex ring;

$$U = \frac{\Gamma}{2\pi D}\left\{\log\frac{4D}{\sqrt{4\nu t}} - 0.558 + O\left[\left(\frac{4\nu t}{D^2}\right)^{\frac{1}{2}}\log\frac{4\nu t}{D^2}\right]\right\} \quad (2)$$

2.2.2 Experimental Research

Krutzsch recorded the translational displacement of the vortex ring. In this research he noted that the displacement follows an e function and therefore plotted the graph using a semi logarithmic scale as shown in Figure 4 (Krutzsch, 1939). His observation that the translation follows an e function was confirmed by additional researchers, as previously explained in regard to deceleration due to viscous diffusion

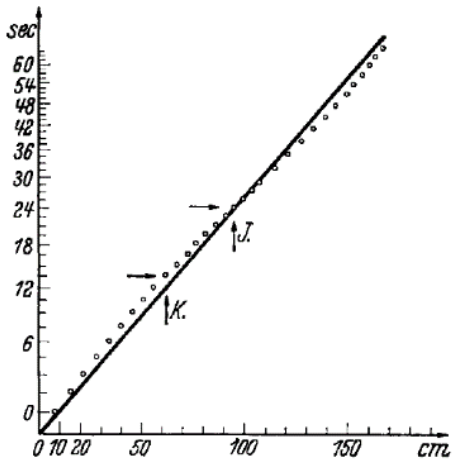

Figure 4 - Translational displacement of Vortex ring (Krutzsch, 1939)

2.3 The Stability of the Vortex Ring

For many decades after the conclusion of Thompson [1867] vortex rings were still observed to be stable. The earliest research showing otherwise was from an experimental study performed by (Krutzsch, 1939). The developing instability is illustrated in Figure 5. His experimental study demonstrated that vortex rings are unstable, however, Krutzsch remarks that the vortex ring must have a very large amount of energy (large Reynolds number) for these instabilities to form. During his study he altered the parameters of formation for the vortex rings, observing the resultant effects on the instability - the mode of the instability, the diameter of the instability, how quickly the instability takes to develop and how long before the instability results in the vortex becoming turbulent. Krutzsch's data is invaluable and has stood the test of time however "Krutzsch attributed the instability to foreign matter acquired from the region outside the orifice during the generation of the ring" (Widnall, 1973), a conclusion which has not been maintained by other researchers.

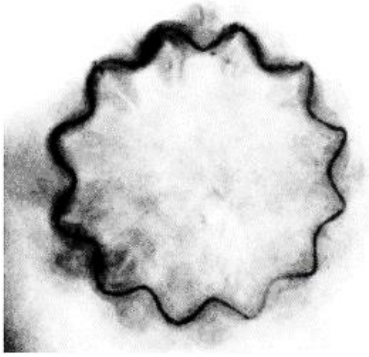

Figure 5 – An instability with a mode of 12 (Krutzsch, 1939)

Although research into the instability of vortex rings was relatively bare, the stability of vortices as a whole had already been delved into by various researchers resulting in stability theory. A specific area of research exploring the stability of vortices was regarding the wake of airplanes. As an airplane moves through the air it produces two contra-rotating vortices in its wake (cf. Figure 6), these vortices can provide issues for other smaller aircraft until they eventually seem to undergo a "slow, symmetric and nearly sinusoidal instability" before turning into a harmless state of turbulent vortex rings (Crow, 1970). Crow established that an irregularity, for example a small gust, would displace the lines slightly and then self-induced motion would amplify this disruption. The wavy pattern is the rapid mutual amplification of this displacement. Crow's model theorised that the self-induced motion was due to each individual element of the vortices affecting every element of the other vortices.

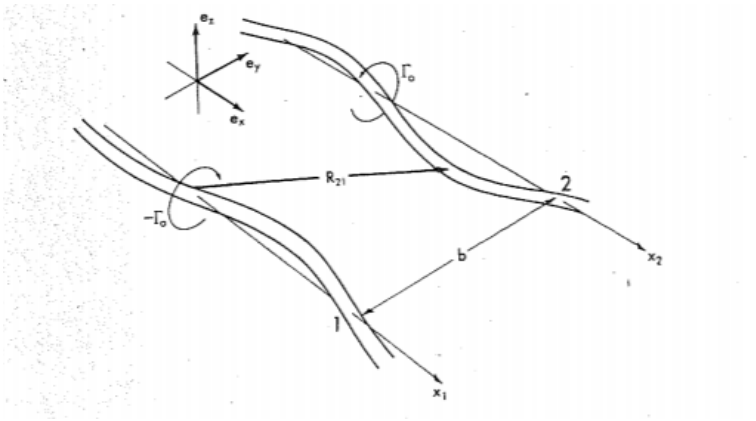

Figure 6 - Trailing vortices of an airplane

While researching the stability of vortex rings, Maxworthy also observed, that like Krutzsch, at a higher Reynolds number the vortex ring becomes unstable (Maxworthy, 1972). Widnall [1973] who had already developed research regarding vortex rings (Widnall, 1971), took a particular interest in the instability of the vortex ring as demonstrated by Krutzsch and Maxworthy. In Widnall's 1973 paper on the stability of vortex rings she investigates this instability, both experimentally and theoretically using concepts of stability theory, then comparing the results. The theoretical research considered "a small vortex filament in regard to the sinusoidal displacements of its centre line" (Widnall, 1973). The experimental research used vortex rings generated in air with smoke to visualise rather than water like Krutzsch, in addition with Widnall using a laser Doppler velocimeter to measure the centreline velocities.

The comparison of results showed a strong agreement in the predicted and actual amplification rates and a weaker agreement between the predicted and actual wave numbers (cf. Figure 7). From this research, Widnall concluded that at high Reynolds numbers, "the vortex ring is unstable to the

sinusoidal displacements of the vortex filaments", in addition to concluding that "the number of waves on the perimeter of the vortex ring increases, as the core size decreases." (Widnall, 1973)

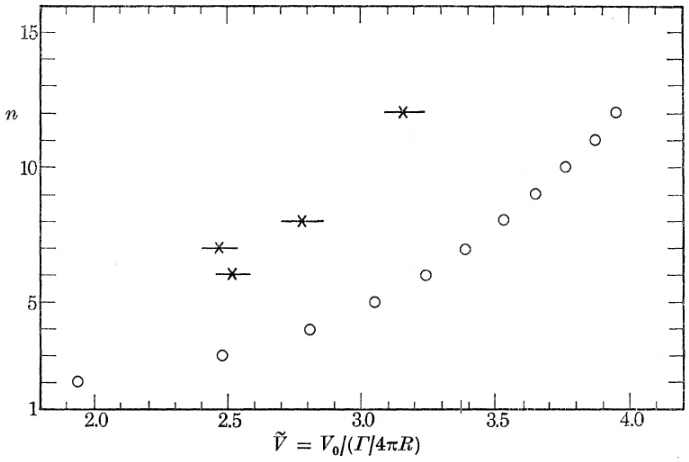

Figure 7 - Number of waves in the unstable mode as a function of $\tilde{V} = V_0/(\Gamma/4\pi R)$; x, experiment; O, theoretical prediction at maximum amplification (Widnall, 1973)

Widnall continued her research, extending her theory of the vortex ring instability to encompass short-wave disturbances (Widnall, et al., 1974) in addition to her more general report on vortex rings in 1975 "The Structure and Dynamics of Vortex Filaments" (Widnall, 1975). The result of Widnall's contribution to understanding this instability resulted in its official name – The Widnall Instability.

Further research into the instability includes Saffman's paper specifically observing the mode of the instability and its dependence on the Reynolds number (Saffman, 1977).

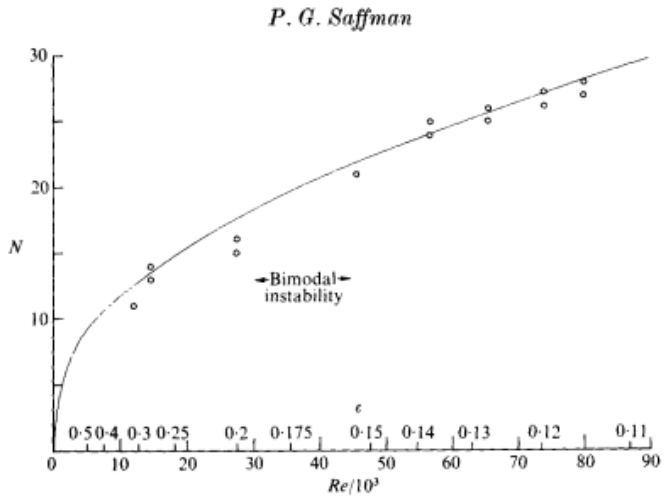

Figure 8 - Dependence of mode on Reynolds number (Saffman, 1977)

He concluded that although there is some disagreement for $3x10^4 < Re < 5x10^4$ where a "bimodal instability is seen to occur", overall there is a clear correlation between the Reynolds number and the mode of the instability (cf. Figure 8).

2.4 Generation of Vortex Rings

The method of generating vortex rings has varied throughout research, Helmholtz's method of forming vortex rings (technically half-rings) consisted of "a circular disk in a fluid suddenly moving normal to the disk surface and then being pulled out of the fluid" (Akhmetov, 2009). A much more common research method of generating impulse vortex rings became pushing a compact amount of liquid out of a circular aperture, this method being used by both Krutzsch and Widnall due to it being easier to analyse the resultant vortex ring.

The common mechanism for this method is an actuated piston in a cylinder. The piston pushes along the fluid within the cylinder, then once this piston reaches the end of its stroke length the accelerated region of fluid continues before being pressed through an opening, usually of which there are two configurations – Nozzle and orifice (cf. Figure 9) (Krueger, 2005).

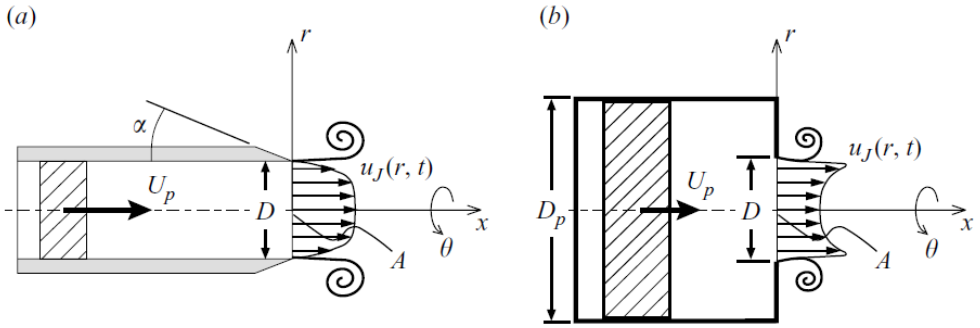

Figure 9 - Different configurations of vortex ring generator (a) Nozzle (b) Orifice (Krueger, 2005)

As the fluid passes through the opening, the boundary layer that has been generated through the length of the cylinder separates at the lip. This boundary layer then becomes a sheet of vorticity (for description of vorticity see 3.2) that rolls up (Krueger, 2005). If the velocity of the fluid is sufficient, the layer curls completely until it is eventually traveling forwards once again. The result is a ring shaped vortex that eventually pinches off the following fluid to produce a detached ring with a thin circular core of circulation propagating forward – a vortex ring.

Study into the formation of vortex rings by (Maxworthy, 1977) clarified that the diameter of the vortex ring is almost always larger than the diameter of the nozzle, and how much larger specifically is based upon the ratio of the stroke length to the nozzle diameter (cf. Figure 10).

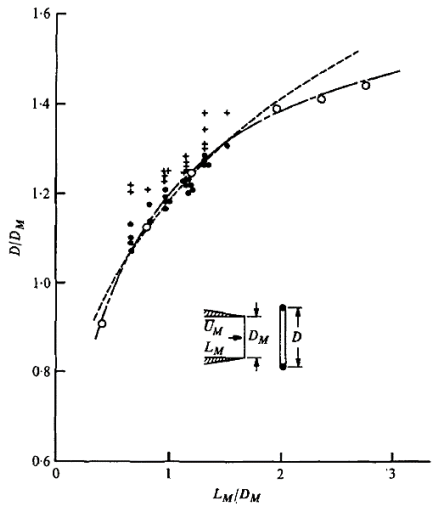

Figure 10 - Ring diameter D/D_m at $2.5D_m$ downstream vs. length of ejected fluid slug L_m/D_m (Maxworthy, 1977)

2.5 Turbulence of Vortex Rings

With the research into the Widnall instability now becoming rather extensive, (Glezer, 1988) began focusing on the form of the vortex rings during formation rather than after. His research consisted of generating vortex rings using various generation parameters, specifically the stroke length of the piston and the piston velocity, testing on two different sized orifices of 1.90cm and 2.54cm. Glezer concluded that whether the vortex ring formed as laminar or turbulent, was approximately based upon two dimensionless variables, $\frac{\Gamma_0}{\nu}$ (J) and $\frac{L_0}{D_0}$.

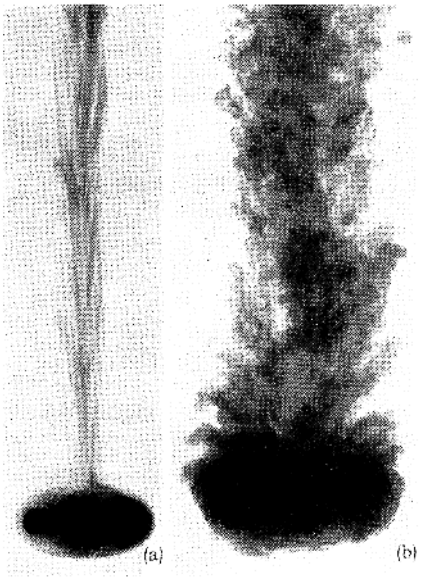

Figure 11 – Photographs of vortex rings using dye for visualisation.
a) the laminar vortex ring at Γ/ν = 7500
b)the turbulent vortex ring at Γ/ν = 27000
(Glezer, 1988)

Glezer observed that during formation of the vortex ring, there seemed to be an instability in the roll up of the cylindrical vortex sheet (cf. Figure 12 circled red) – comparing this to the Kelvin-Helmholtz instability of a free shear layer.

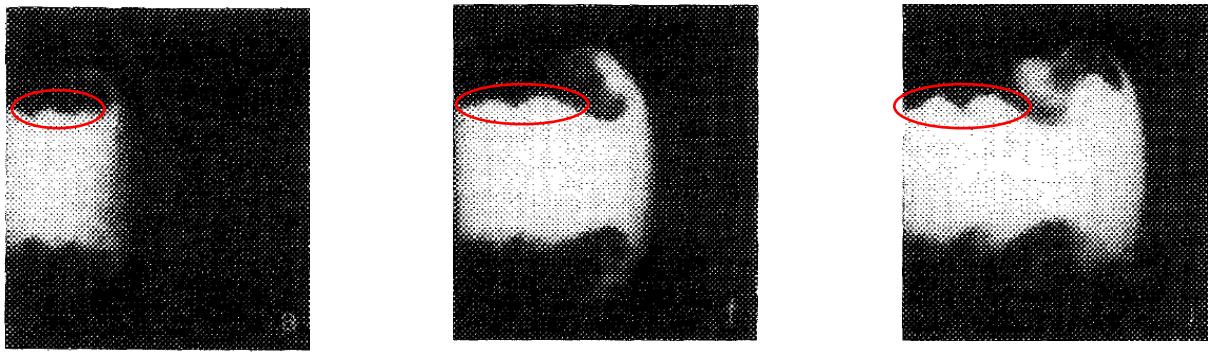

Figure 12 -Instability during the formation of a vortex ring (Glezer, 1988)

Glezer also observed that for a fixed $\frac{L_0}{D_0}$, the distance before an initially laminar vortex ring became turbulent decreased as the piston velocity increased (Glezer, 1988). This was also observed by previous research such as (Maxworthy, 1977) who noted that both the onset and breakdown of the instability occurred closer to the generator when the Reynolds number of formation was increased. Glezer concluded that it was reasonable conjecture that disturbances introduced by the previously mentioned instability of the vortex sheet roll up, could "accelerate the onset, amplification and breakdown to turbulence of the azimuthal core instability."

2.6 ALTERNATIVE SHAPES OF FORMATION APERTURES

Eventually, research into different shapes of vortex rings became a field of interest to many researchers. For example, (De Bernardinis & Dhanak, 1981) researched into the characteristics of a vortex ring formed from an elliptical aperture. They specifically focused on developing theoretical predictions for the behaviour of the ring, then to compare it with experimental measurements. The recorded data showed the elliptical ring to oscillate, and depending on the size of the shape, these oscillations would either last periodically or break up into multiple rings.

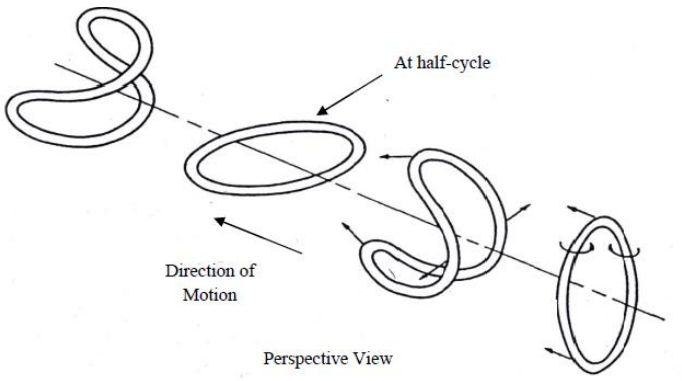

Figure 13 – Oscillations of elliptic vortex rings (Adhikari, 2009)

More recent research (Huang & Chan, 2007) explored changing the form of the aperture to an elliptical, triangular and even hexagonal orifice to observe the resulting affects. Huang and Chan observed that the elliptical aperture of higher Reynolds numbers in addition to the triangular aperture both showed the Widnall instability, however, the hexagonal aperture unfortunately, although shifting during motion, did not conclusively show the Widnall instability.

2.7 APPLICATIONS OF VORTEX RINGS

Research into the practical applications of vortex rings, include the development of a “smart pill that would use mini vortex ring turbines as propulsion to travel throughout the digestive tract, identifying and treating disease” (Gorder, 2004). They have also provided more efficient methods of fighting gas and oil fires, the original idea of Lavrentev and the Siberian Branch of the USSR Academy of Sciences [1973] - extinguishing the fires via an explosion-induced vortex ring, further researched for an explanation of the flame quenching mechanism by (Akhmetov, et al., 1980)

2.8 CONCLUSION

There has been a vast amount of research into the translational velocity and instability of vortex rings, in addition to more recent research into alternative apertures and their resulting affects. Attempting to specifically impose an alternative instability however appears to be untested. This is most likely due to the fact that accurately developing a nozzle with an aperture of a specific waveform has only recently been made possible due to developments in 3D printing.

3 THEORY

The following section will consist of some of the core knowledge and equations involved in regard to discussing fluid dynamics, specifically vortex rings.

3.1 REYNOLD'S NUMBER

As mentioned in the literature review, (Krutzsch, 1939) mentioned that the instability only forms within vortex rings of high energies, i.e having a high Reynolds number. The Reynolds number is a dimensionless quantity popularised by Osbourne Reynolds (Reynolds, 1883). The quantity represents the ratio between the inertial force and the viscous force.

$$Re = \frac{\rho V D}{\mu}$$

Where the ρ represents the density of the fluid, V represents the velocity of the fluid, D represents the reference length of the system and μ represents the dynamic viscosity of the fluid.

For this experiment, although they are very much related, technically the Reynolds number pre and post ejection are different. Therefore, two versions of Reynold's number are defined – The Reynolds number or the piston and the Reynold's number of the vortex ring.

3.1.1 Pre - Ejection (Piston) Reynold's Number

This considers the fluid just before ejection after being accelerated by the piston. The reference length used is the stroke length L and the velocity used is the piston velocity U_P.

3.1.2 Post – Ejection (Ring) Reynold's Number

This is the Reynold's Number after departing the aperture, once the roll up has completed, producing a full detached vortex ring. The reference length used is the diameter of the vortex ring D and the velocity used is the velocity of the vortex ring U.

3.2 VORTICITY

The vorticity (ξ) of a fluid is defined as two times the angular velocity vector (ω).

$$\xi = 2\omega = curlV$$

It represents a measure of the swirling motion of the fluid and is a key component in explaining various aspects of the vortex ring, specifically the roll up of the sheet of vorticity producing the ring. For further details refer to, for instance, (White, 2008).

3.3 CIRCULATION

Irrotational flow is flow that has a vorticity of zero and thus an angular velocity of zero. In this type of flow, however, it is common for translational rotation of fluid elements in a circular motion, without the orientation of the element changing in regard to the entire system. This aspect of the flow is connected to the quantity know as circulation.

Formally, the circulation Γ denotes the "net algebraic strength of all the vortex filaments contained within the closed curve" (Akhmetov, 2009), where this is calculated using the counter clockwise line integral, around a closed curve C, of arc length Ds times the velocity component tangent to the curve:

$$\Gamma = \oint V \cos\alpha \, ds$$

Experimentally, the circulation is calculated slightly differently, either by using a specialised piece of equipment or commonly simply using the "slug model" estimation (Krueger, 2005)

$$\Gamma_{sm} = \frac{1}{2}\int_0^{t_p} {U_P}^2(t)dt \quad (3)$$

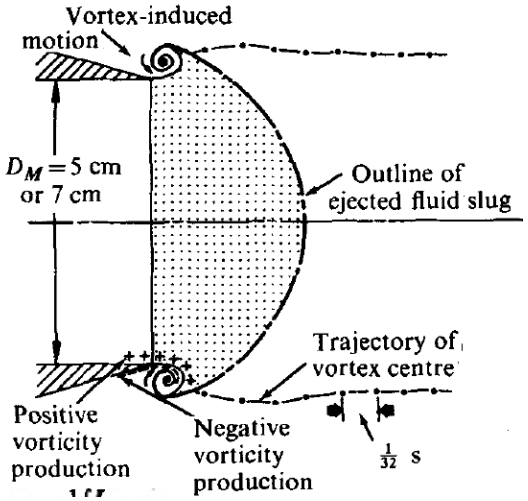

Figure 14 - Slug Model Approximation Diagram (Maxworthy, 1977)

3.4 TURBULENT AND LAMINAR FLOW

Flow can either be laminar or turbulent. Laminar flow is flow that follows a smooth predictable pattern modelled as thin sheets (laminas), sliding over one another. Turbulent flow is disorganised flow consisting of many eddies continuously mixing etc. superimposing to produce a forward motion, however, on a deeper analysis the individual flows are very difficult to predict. As the Reynolds number is increased, flow tends to become more turbulent.

4 METHOD

4.1 EXPERIMENTAL SETUP

The test rig was composed of various components. The core structure of the apparatus was the large extended water tank repurposed from a previous project. In addition to this tank, a piston-cylinder vortex ring generator was also utilised. Other parts such as the base plate to secure the vortex ring generator, as well as the pulley system that actuated the piston, were both designed and built in the workshop as adaptations to the existing rig to facilitate the proposed method. Apparatus once fully set up appears as Figure 15.

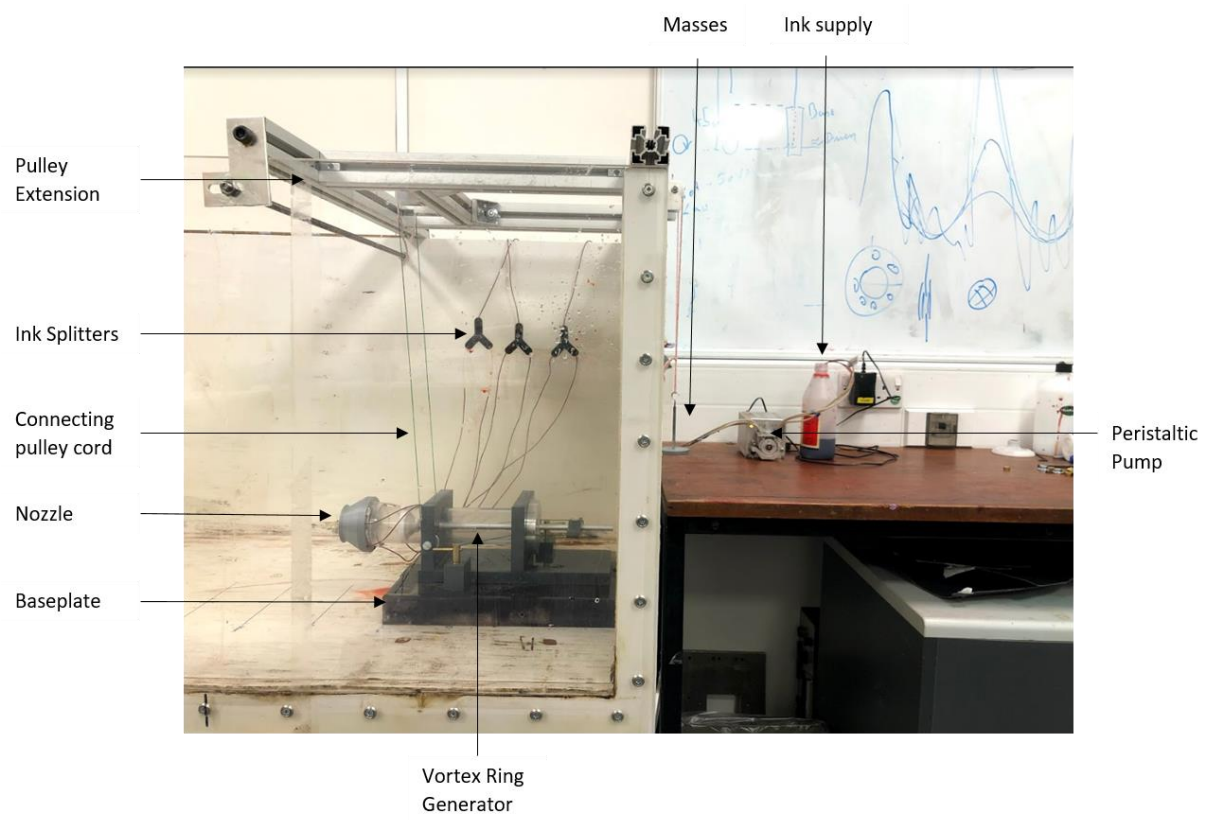

Figure 15 - Apparatus configuration

4.1.1 Vortex ring generator

The piston-cylinder vortex ring generator was acquired from a previous project (Mansi, 2019) due to its suitability to this project. This previous project was studying vortex rings in the air, however, as this didn't work that well, it was proposed to test it in water where if the visualisation techniques of dye were administered correctly, it would be a lot clearer to see the resultant rings.

The cylinder design incorporates magnets in the generation end (left side of Figure 17) for easy attachment of nozzles; due to the proposed method of testing this project, the ability to easily change nozzles simply via magnets was invaluable. The apparatus also had a mechanical system of actuation (cf. Figure 16), a lot simpler and safer than the electronic alternative, this was deemed ideal for the project.

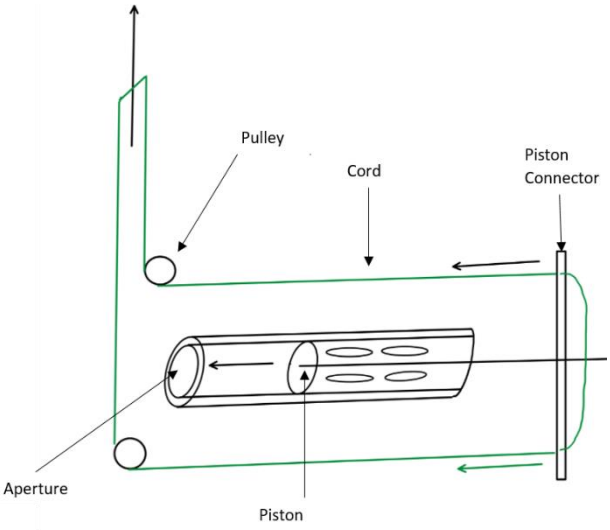

Figure 16 - Diagram illustrating mechanism of actuation

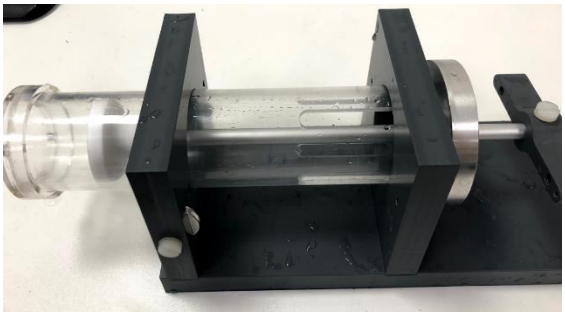

Figure 17 - Vortex Ring Generator

As the distance of the pulley system was not feasible for the designed usage, an extension (red sketch in Figure 19) to the system was developed to facilitate the actuation from masses well outside of the water tank. The fully assembled extension is shown in Figure 18.

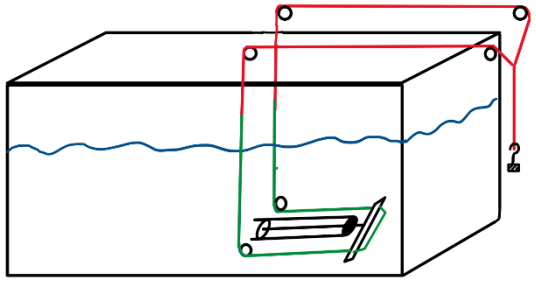

Figure 19 - Diagram illustrating piston extension

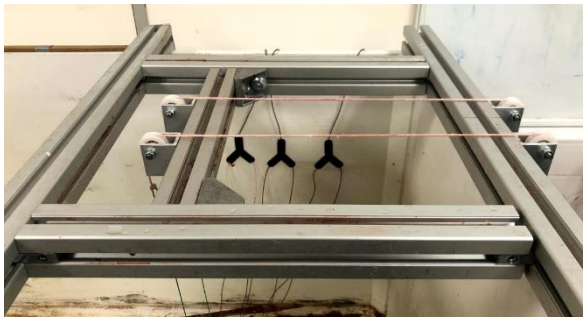

Figure 18 – Extended Pulley System

4.1.2 Base plate

Due to the weights providing a moving force to the pulleys and thus the apparatus as well, a heavy support structure was developed. The base plate has 2 clamps that hold the frame of the vortex ring generator firmly. This ensures that during actuation, the weight of the mass does not provide enough force to displace the vortex rings generator/ vortex rings during generation. (cf. Figure 20)

Figure 20 - Base plate

4.1.3 Water tank

The water tank was used in a previous experiment exploring the Widnall instability and is therefore designed with these observations in mind (Burk, 2011). The tank is 2m long, specifically made long enough to ensure the instability can form and be observed via its 2 transparent walls. In addition to this, the tank has distance markings along its base to allow the user to measure the speed of the vortex rings.

4.1.4 Input splitters

The peristaltic pump used for ink injection only had three outputs. During the design phase of the nozzle, a simple three input design was tested, however, did not achieve the uniform dispersion required. Therefore, it was proposed to double the number of ink inputs to six equally spaced inputs to assist in achieving a more uniform distribution. To facilitate six inputs, it was necessary to design and 3D print splitters to divide the three inputs into six.

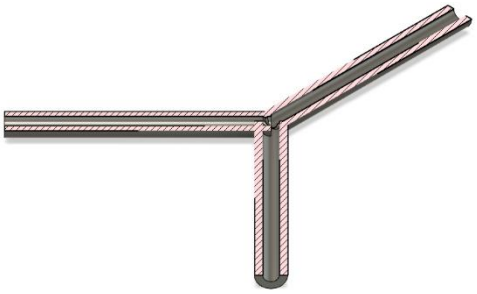

Figure 21 - Isometric section-view of ink splitter

4.1.5 Calibrating the buoyancy of the ink

Although the buoyancy of the ink was not a crucial parameter during testing, the tests still required a relatively neutrally buoyant ink. This helped preserve the distribution of the ink around the nozzle (rather than all sinking to the bottom of the nozzle/floating to the top of the nozzle), in addition to ensuring that the vortex rings travelled far enough down the tank to observe them effectively. Often, after a few tests the vortex rings would be seen to start rising/sinking during travel, resulting in the need for the buoyancy to be adjusted again. When necessary, fresh ink would be mixed with overly buoyant ink in a separate container. The buoyancy of the new ink mixture would then be estimated by slowly injecting a small amount horizontally into the tank and observing the motion of the ink, i.e. once mixed correctly, remaining at a neutral level in the tank.

4.2 NOZZLES

4.2.1 Standard circular nozzle

Following the implementation of magnets in the previous project's nozzles/cylinder, this idea was preserved in the new designs ensuring to include 6 equally spaced holes for insertion of magnets at the base of the nozzle (cf. Figure 22).

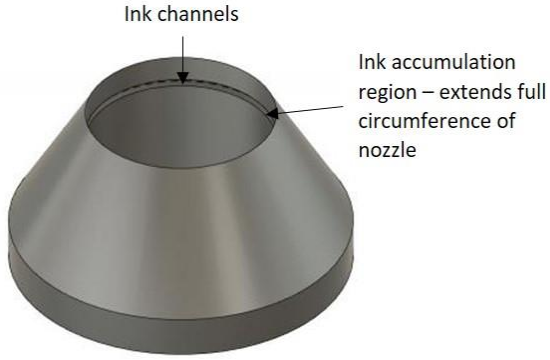

Figure 23 - Isometric view of designed circular nozzle

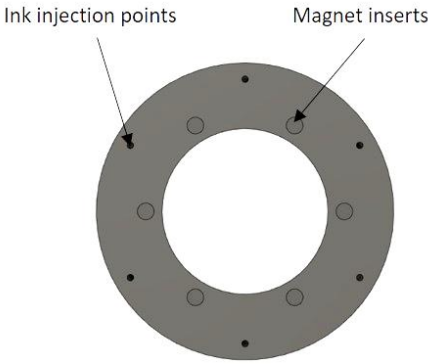

Figure 22 - Bottom view of nozzle displaying 6 ink inputs (outer) and 6 magnet inserts (inner)

As the previous project produced vortex rings in air, the nozzle did not have to facilitate ink injection and was simply a solid structure with an aperture. For this project, ink injection had to be considered and therefore, the internal structure of the nozzle redesigned. This redesign involved the nozzle housing many thin ink channels travelling from the back/base of the nozzle to a small opening (ink accumulation region) approximately 5cm from the front of the nozzle (cf. Figure 23). A peristaltic pump with an ink supply was connected to the ink inputs, ink was then injected forming a uniform distribution extending the entire ink reservoir (cf. Figure 24). Then the ink passed through ink channels before re-joining in the ink accumulation region and being released as a thin uniform layer just before the opening of the nozzle – optimal conditions for the visualisation of the vortex ring.

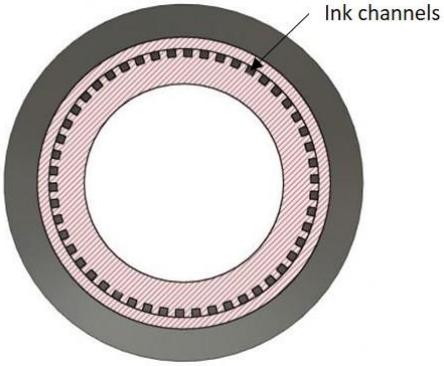

Figure 25 - Plan section view displaying the 50 thin ink channels extending the nozzle

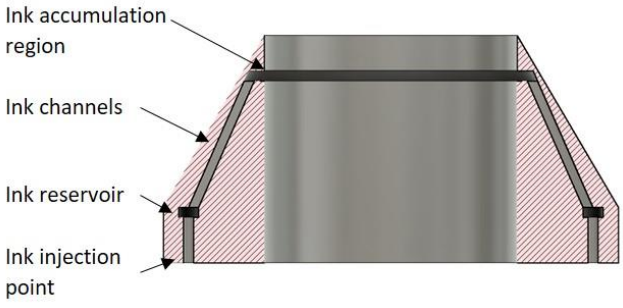

Figure 24 - Cross-section view displaying the path of the channels from the base to ejection

4.2.2 Wavy Nozzle

Once the control testing of the system had been completed ensuring that it could produce clear consistent vortex rings with an observable Widnall instability, the design of the wavy nozzle began. The wave form of the recorded instabilities were noted and the previous nozzle design was adapted based on this. The nozzle's aperture was adjusted to have an opening of the same shape/waveform/wavenumber as a naturally occurring instability (see forward to results section 5.2 - Figure 40 B). This was done by superposing a picture of the instability as a canvas onto the aperture of the nozzle, from this it was then possible to use splines to copy the shape, then extruding it through to join the nozzle.

4.2.2.1 1st iteration

The first iteration of the nozzle design provided some successful results however a key design flaw was noted – the large lip before the aperture (highlighted red Figure 26). Discussing the lip, it was brought to attention that this lip would disrupt the boundary layer and therefore interfere with the roll up of the boundary layer to produce the vortex ring. Also, due to the design method of this nozzle, its diameter was slightly smaller than the standard circular nozzles diameter

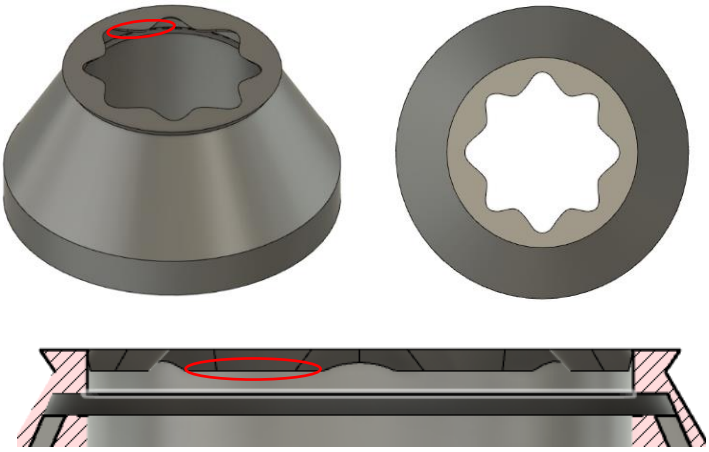

Figure 26 – 1st iteration of wavy nozzle

4.2.2.2 2nd iteration

To improve the design it was proposed to incorporate a smooth transition into the aperture thus removing this potentially interruptive lip. The goal of this design was to try and help preserve the boundary layer therefore facilitating better roll up and producing clearer and more consistent vortex rings. In addition, this design method also facilitated ensuring the average diameter was approximately the same as the circular nozzle, thus making it easier to compare the results of the two nozzles.

Figure 27 – 2nd iteration of wavy nozzle

4.3 EXPERIMENTAL PROCEDURE

4.3.1 Testing

The beginning of this project involved confirming that the apparatus could produce consistent clear vortex rings with an observable Widnall instability. The core apparatus was set up as shown in Figure 15. A nozzle with a standard circular aperture (cf. Figure 22) was printed and via the implanted magnets, attached to the cylinder head. The piston was pulled back raising the end of the pulley system above the ground. The peristaltic pump was connected using pipes inserted into the base of the nozzle (cf. Figure 22); the pump was switched on slowly delivering ink into the nozzle head. The base plate was checked to be securely fastened to the cylinder frame before the weights were released at the raised end of the pulley system. This exerted a quick impulse across the system to the piston, shooting forward, squeezing the compact volume of water and ink out as a visible vortex ring. For the testing of the wavy nozzle, the nozzle was swapped and the same procedure was repeated.

4.3.2 Parameters

Various parameters were tested in order to try and determine a range of optimal conditions for the formation of vortex rings with a clear Widnall instability. The stroke length of the piston (how far back the piston was pulled before ejection) and the speed of the piston head (how much weight was used to pull the piston) were both adjusted observing the resultant vortex rings.

(Krutzsch, 1939) had already noted a rough ranges of values that were known to work so testing began within these ranges until eventually a rough set of values were noted – keeping the stroke length at 5cm and varying the weights from 50g to 200g. In Krutzsch's paper, the diameter of the aperture was also adjusted however this was kept at a constant value known to be viable for ring production (5cm) throughout the nozzles.

Rohrdurchmesser 7,6 cm

Nr.	Kolben-stoß-länge in cm	Kolben-geschw. in cm/sec	Reyn. Zahl	Zeit bis Kröpf. in Sek.	Zeit bis Inst. in Sek.	cm bis Kröpf.	cm bis Inst.	Kröp-fungs-zahl	Durch-messer des Ringes in cm
1	2,13	11,0	3810	12,2	38,2	30,8	75,0	7	5,6
2	3,30	11,4	3880	12,5	31,0	33,5	72,2	8	6,8
3	5,05	10,8	4110	18,5	41,5	50,7	100,2	6	8,2
4	5,70	11,0	3800	14,0	24,0	44,0	93,5	7	8,2
5	8,97	10,9	3770	12,0	18,0	45,0	76,3	9	9,4
6	3,20	13,5	5110	3,0	20,0	7,5	70,0	8	8,8
7	9,33	13,9	5270	9,0	17,0	36,5	73,7	10	9,4
8	4,10	18,9	7180	4,5	15,5	30,0	70,5	10	7,6
9	6,25	18,4	7000	4,0	14,0	30,0	73,0	10	8,8
10	8,08	19,2	7300	5,0	13,0	32,2	80,5	12	9,2
11	2,30	19,1	7250	3,5	13,5	15,0	57,5	8	5,6
			Rohrdurchmesser 3,0 cm						
12	2,20	10,2	1530	24,0	—	40,5	—	3	3,1
13	5,93	9,7	1460	5,5	13,0	19,0	40,0	6	3,8
14	7,50	9,8	1473	5,0	9,5	18,5	33,6	6	4,0
15	2,95	13,7	2050	11,5	22,0	36,0	57,5	6	3,5
16	7,55	13,8	2075	3,0	6,0	15,3	31,2	6	4,2
17	8,95	13,7	2050	3,0	4,5	17,0	25,0	7	4,3
18	2,15	16,7	2505	7,0	17,0	24,3	48,3	6	4,0
19	4,35	16,5	2470	3,0	6,0	16,0	29,5	8	3,8

Table 1- Krutzsch's data (Krutzsch, 1939)

4.4 RECORDING

4.4.1 The traversing vortex ring

The traversing propagation of the rings was deemed a key constituent to the study of the dynamics of vortex rings and therefore was recorded. This was tested by filming the tank from the extended side to provide a full view of propagation. There was a measuring apparatus placed into the tank, close to the path of the vortex ring, to provide a measurement of the distance from ejection. The measuring apparatus used was a long thin strip of wood that had been marked every 10cm. It had been clamped at one end and weighted at the other end.

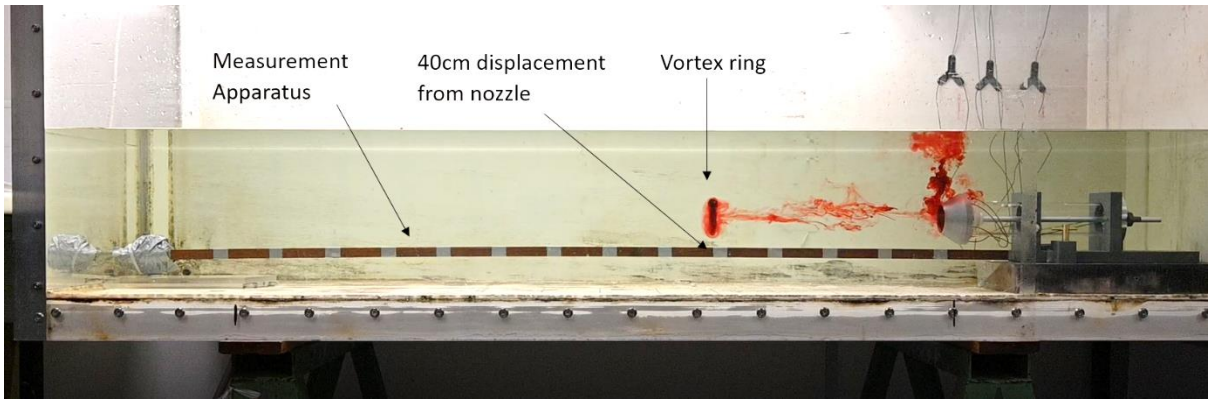

Figure 28 - Translational velocity measurement apparatus

4.4.2 The full view full of waves

To record the face of the vortex ring and its respective number of waves, diameter and core radius, the vortex ring was filmed from the end of the tank, perpendicular to the direction of motion. After the ejection of the vortex ring, a blank waterproof board was placed well behind the vortex ring to ensure no disruption, however, provide a blank background for the vortex ring formed to be analysed clearly.

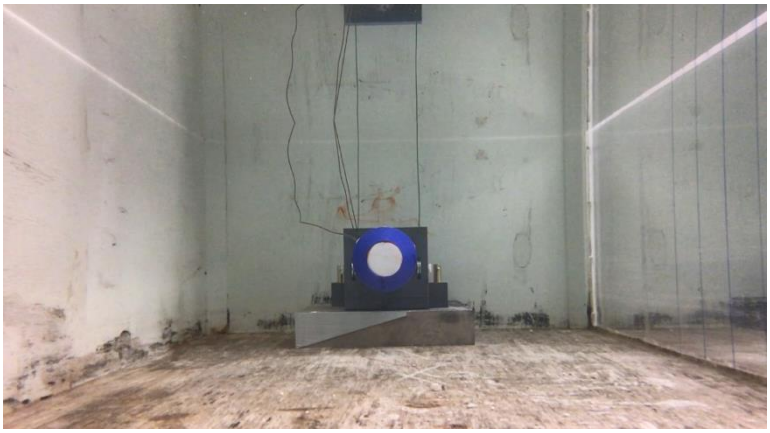

Figure 29 - The view from the Face-on recordings

4.4.3 Measuring the velocity of the piston

As explained in 3.1.1, velocity is a key component in calculating the Reynolds number. In Krutzsch's paper (Krutzsch, 1939), it is shown that there is a clear correlation between the form of the vortex ring and the Reynolds number of the fluid. Therefore, the piston velocity was deemed a necessary characteristic to calculate. Due to the complications of calculating it theoretically, it was calculated experimentally, however, as it would have been difficult to measure the piston specifically, the velocity of the weights was measured instead as due to the tension in the pulley system, they are equivalent. The velocity of the falling weights was measured in a similar method to the velocity of the rings, recording the displacement of the weights and performing frame by frame analysis to compare this displacement with the time code of the frame, once plotted thus providing the velocity.

Figure 30 - Measuring speed of weight drop

4.4.4 The Diameter of the vortex ring

The diameter of the vortex ring was calculated using a pixel ruler (RapidTables, 2016). For calibration, a still from the beginning of the video was taken and measured (cf Figure 29). This still was ensured to be taken before ink injection and therefore, clear to analyse. The number of pixels corresponding to the diameter of the nozzle was then recorded.

For each video recording the face of the waves, a still was taken where the edges could be relatively clearly defined, and therefore a reading for the number of pixels extending the diameter of the ring measured. The ratio of this measurement compared to the known number of pixels/diameter measurement from the calibration photo, allowed for a fairly reliable estimation of the vortex ring diameter.

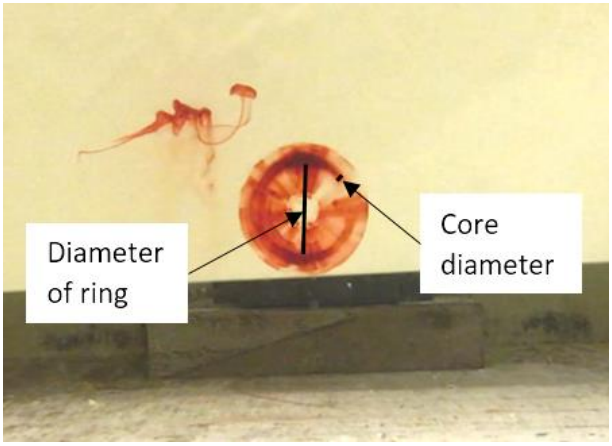

Figure 31 - Diameter measurements of Vortex Ring

5 RESULTS

5.1 TRANSLATIONAL VELOCITY

5.1.1 Circular Nozzle

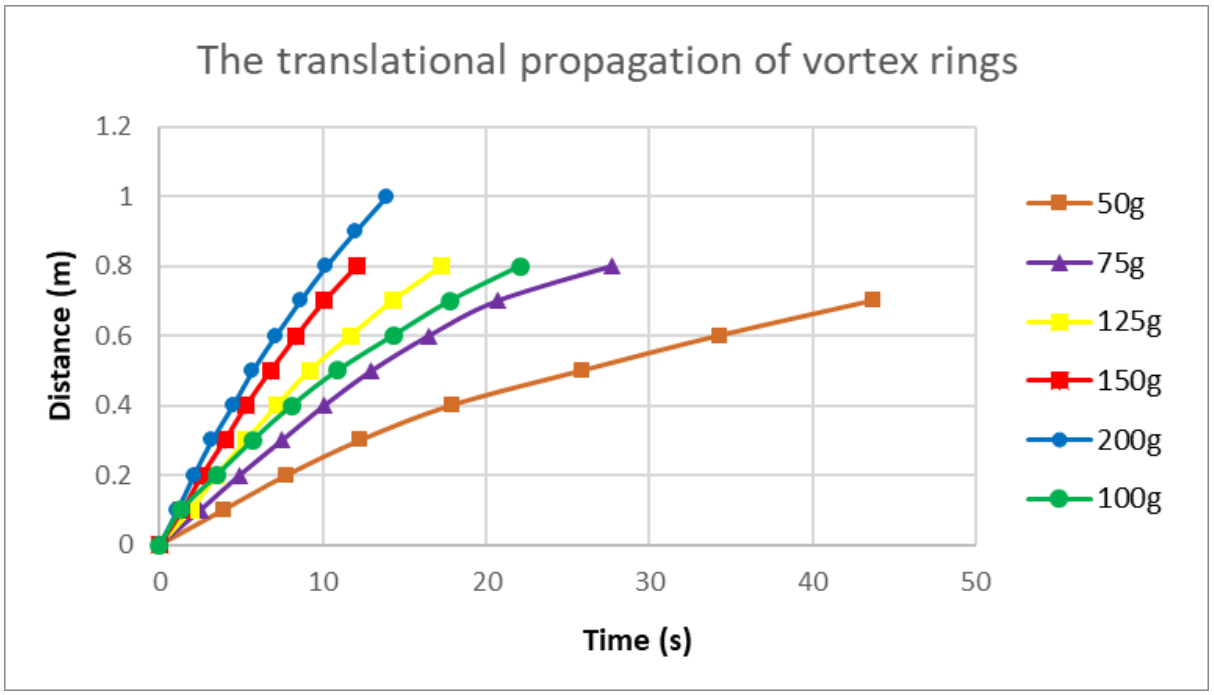

Figure 32 - The translational propagation of vortex rings

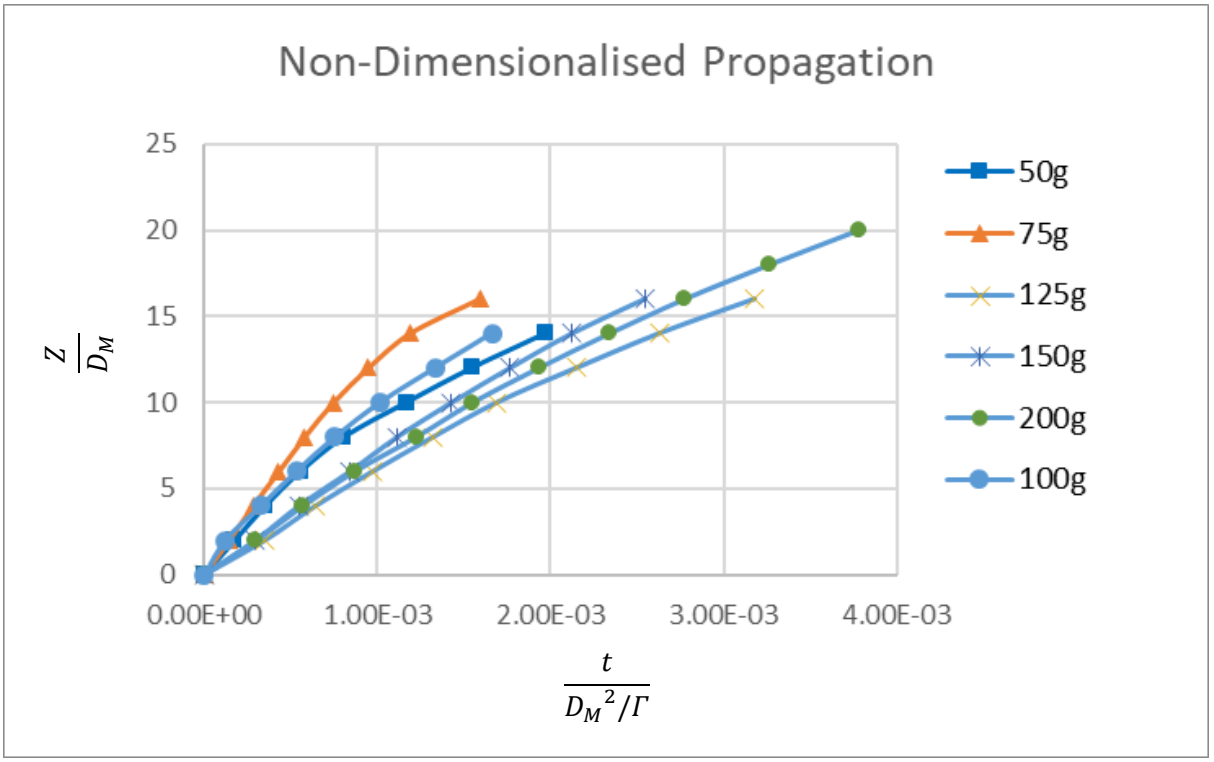

Figure 33 - Non-Dimensionalised translational propagation of vortex rings

5.1.2 Wavy Nozzle

The translational velocity of the circular nozzle was compared with the translational velocity of the wavy nozzle. The trend consistently shown in each plot indicated that the vortex ring produced by the circular nozzle was slightly faster than the vortex ring produced by the wavy nozzle.

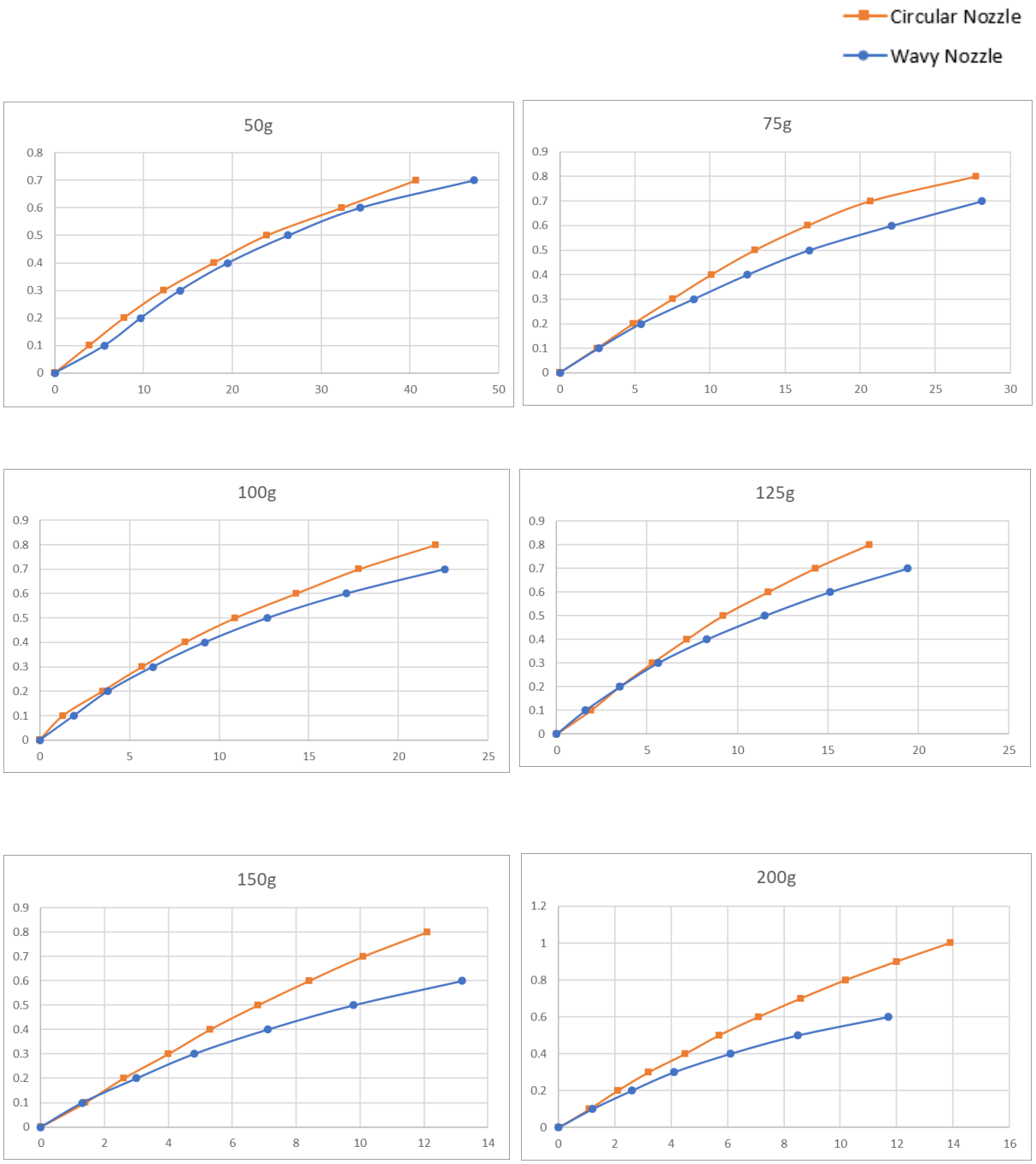

Figure 34 – Velocity comparisons between rings produced by a circular nozzle and wavy nozzle

It was also noted that for the majority of the tests, the vortex ring produced by the wavy nozzle appeared to decelerate faster. In addition to this, the disparity between the lines seems to increase as the load was increased

5.1.3 Parallax error

To confirm whether the parallax error would have a significant effect on the accuracy of the results, a picture was taken with a second ruler placed directly in line with the potential vortex ring, therefore having no parallax error. The rulers were then compared to gauge the difference between the readings, with and without a parallax error, thus gauging the severity of the parallax error. The difference was calculated using a pixel ruler (RapidTables, 2016).

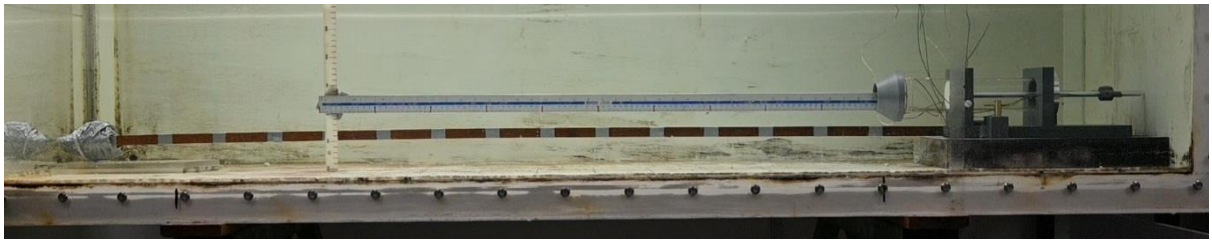

Figure 35 – Calibrating parallax error of measurement apparatus

The maximum disparity in the pixels, located at either end of the tank, was less than 10 pixels, the equivalent of less than a centimetre error. This difference became vastly smaller as the vortex ring approached the middle region of the tank. As the far left of the tank was rarely needed due to the rings often decaying before reaching it, the only parallax error included was just after ejection. Due to the small magnitude of this error, it was considered acceptable as the proposed method of measuring the placement of the rings in regard to the markers, will incorporate an unavoidable error of similar magnitude.

5.1.4 Repeatability testing

To test for other potential errors within the recordings, the experiment was repeated 3 times for various masses – 100g, 150g and 200g. This was used to gauge the repeatability of the experiment and confirm the quality of the data.

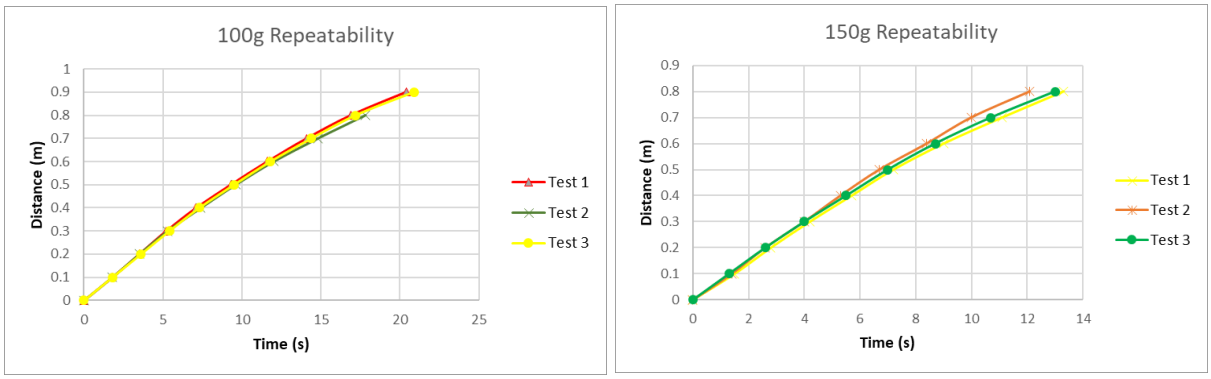

Figure 36 - Repeatability testing for 100g and 150g

Each series of tests showed strong repeatability as each of the three tests produced almost identical results. The standard deviation of the plots generally grew as the time increased, as expected due to prolonged exposure to uncontrollable varying factors such as the motion of the water. The greatest deviation of the 100g, 150g and 200g plots was 0.42s, 1.31s and 0.16s respectively. This error is very small in the scale of factors and therefore was considered negligible

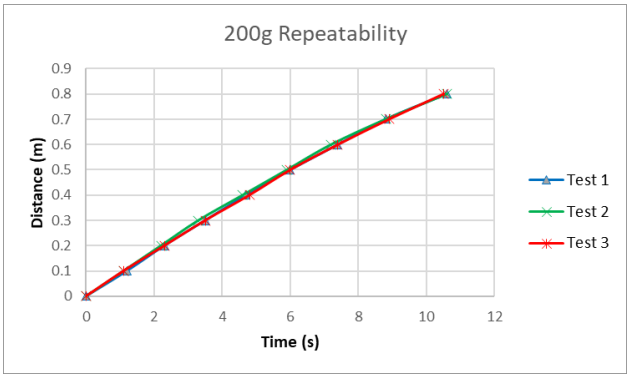

Figure 37 - Repeatability testing for 200g

5.1.5 Potential error of ruler left near vortex ring

It was proposed that the measuring apparatus within close vicinity to the travelling vortex ring (cf. Figure 28) could potentially disturb the vortex ring. For this reason, testing was performed measuring the velocity, with and without the ruler, to confirm that the ruler did not affect the motion of the vortex rings. To record the data without the ruler, a picture of the apparatus with the ruler was taken and then without the camera being moved, the ruler was removed and the propagation of the vortex ring was recorded. The picture was superposed onto the video as a semi-transparent image, and as before, the distance along the ruler was compared against the time in order to plot the velocity. This plot was then compared to the previous plot of the same generation conditions.

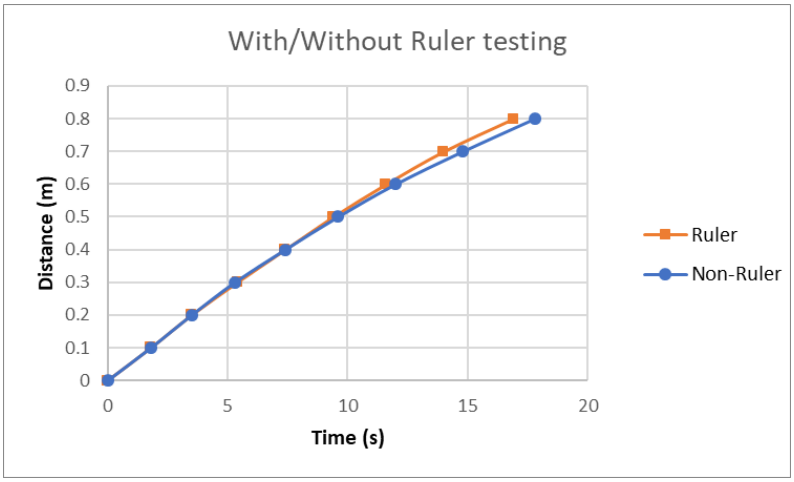

Figure 38 - Testing of 100g with and without the ruler present

As shown in Figure 38, the disparity between the two plots is no different to the standard repeatability testing. For this reason, it was deemed that the ruler had no acknowledgeable effect on the velocity of the vortex rings for the purpose of this project.

5.2 THE FORM OF THE INSTABILITY

5.2.1 Growth of the Instability

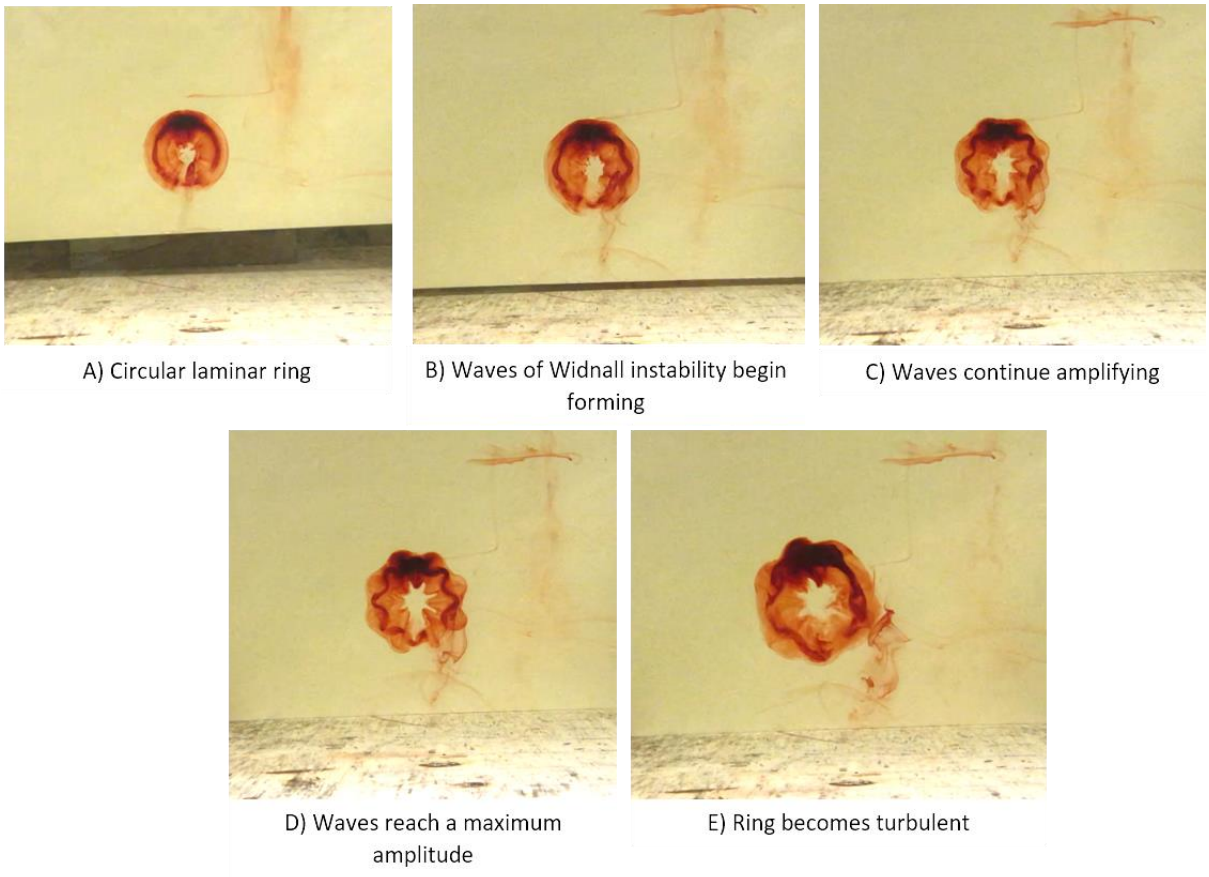

Figure 39 - Gradual Formation of Instability with a mode of 8

5.2.2 Mode of the instability

The mode of the instability was recorded for each of the experiments. Often the ink dispersion was not perfect however it was possible to infer the mode if the majority of the form was clear. Some of the clearest pictures of the instability have been included below.

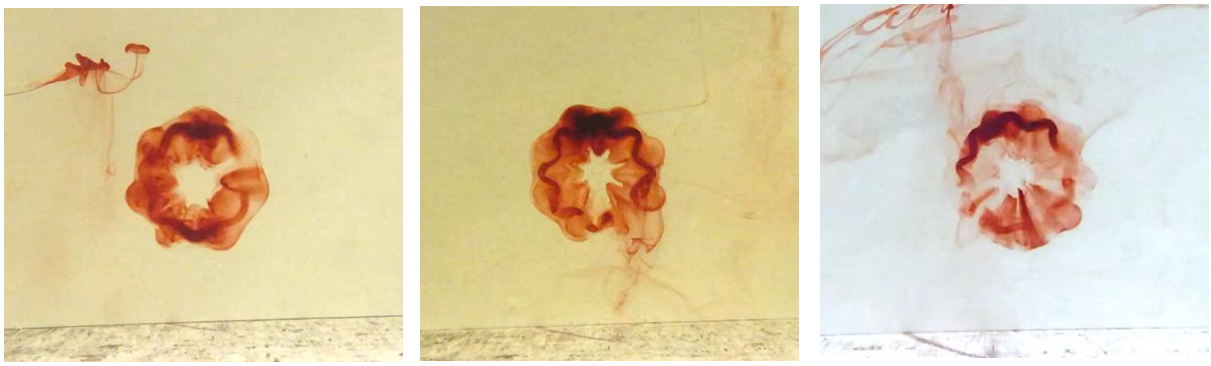

Figure 40 - Instability formed with various modes. A) 7 B) 8 C) 9

5.3 DISTANCE BEFORE TURBULENCE

The point at which the instability was a maximum, just before becoming turbulent and therefore easiest to see, was noted.

Nr.	Mass (g)	Circular Nozzle	Wavy Nozzle
1	50	68	/
2	75	48	48
3	100	43	40
4	125	40	/
5	150	40	40
6	200	38	/

Table 2 - Distance before turbulence for Circular Nozzle Vs Wavy Nozzle

Due to the added turbulence of the wavy nozzle, it was not always clear where the instability became turbulent or whether there even was an instability. For the recordings that clearly showed the point of transition from a Widnall instability to turbulence, the distance before transition remained relatively consistent with the corresponding vortex rings of the circular nozzle. The small disparity between the 100g data sets is comparable with the repeatability testing disparity (cf. Table 4). For this reason it was concluded that the change of nozzle has no significant effect upon the formation of the instability.

5.3.1 Potential error of the ruler near the vortex ring

The recordings of with/without the ruler were compared to confirm that other parameters such as the distance before instability induced turbulence were also not affected by the ruler. As shown in Table 3, there is clearly no effect.

	Distance before instability induced turbulence (cm)
With Ruler	43
Without Ruler	43

Table 3 – 100g With/Without ruler testing

5.3.2 Repeatability of instability induced turbulence

The repeatability of the distance before instability induce turbulence was also checked for various generation parameters. The variation of Table 4 was deemed valid

	Repeat 1	**Repeat 2**	**Repeat 3**
100g	43	40	45
150g	43	40	40
200g	40	38	35

Table 4 - Repeatability testing of instability formation

5.4 Piston/Weight Velocity

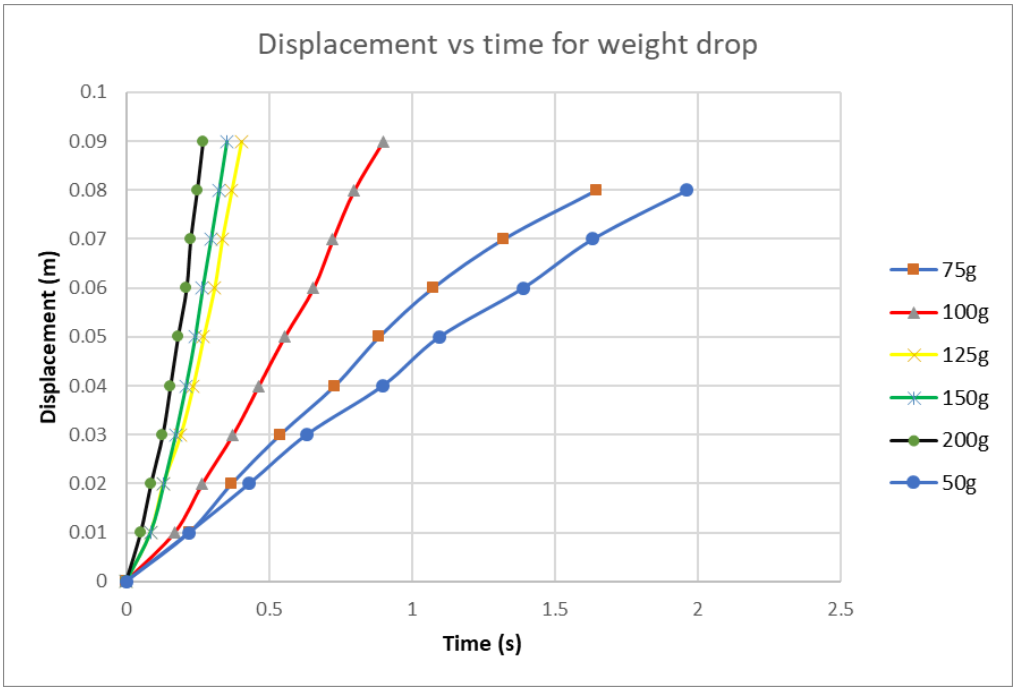

Figure 41 - Displacement vs time plot for weight drop

5.5 Instability Data

The key characteristics of each vortex ring were noted and tabulated to form Table 5.

Stroke length: 5cm

Nozzle Diameter: 5cm

Nr.	Mass (g)	Piston Velocity (cm/s)	Ring Velocity (cm/s)	Diameter of Ring (cm)	Distance to Instability - Turbulent transition (cm)	Reynolds Number of ring R_r	Reynolds Number of formation R_p	Number of waves
1	50g	4.1	1.7	6.6	68	1260	2300	6
2	75g	5.1	3	6.6	48	2220	2860	7
3	100g	10.42	3.6	6.2	43	2500	5840	8
4	125g	22.87	4.7	6.2	40	3270	12820	9
5	150g	26.73	6.7	6.2	40	4660	14990	10
6	200g	33.82	7.2	6	38	4840	18960	12

Table 5 – Circular Nozzle Instability Data

5.6 IMPOSING AN INSTABILITY

Both nozzles produced a wavy configuration as shown in Figure 43 and Figure 42. In both cases, the wavy configuration was observed to match the same form as the nozzle, specifically – 8 waves.

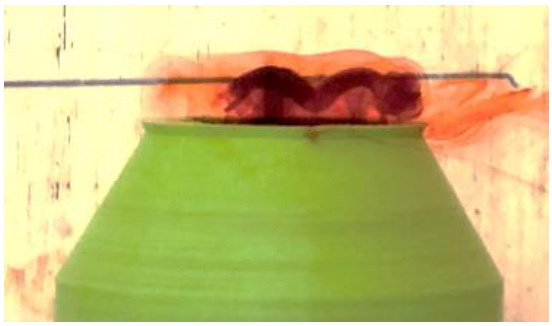

Figure 42 – 1st iteration nozzle - shape production

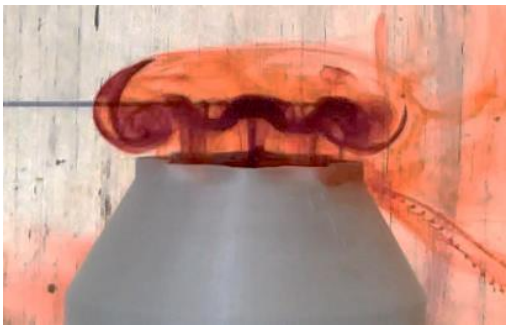

Figure 43 – 2nd iteration nozzle - shape production

Once this shape had been produced, there were often 2 scenarios. The first of the scenarios, more frequently observed, was the quick decay of the wavy configuration before the ring became turbulent. The second scenario observed the initial wavy shape being preserved slightly longer before the ring returned to a relatively standard circular vortex ring. Once the ring returned to a circular shape it followed a similar process to previously generated rings, after a certain distance showing signs of the Widnall instability before it was amplified to such an extent the ring became turbulent. This transition from the wavy shape – circular – Instability is shown in Figure 44.

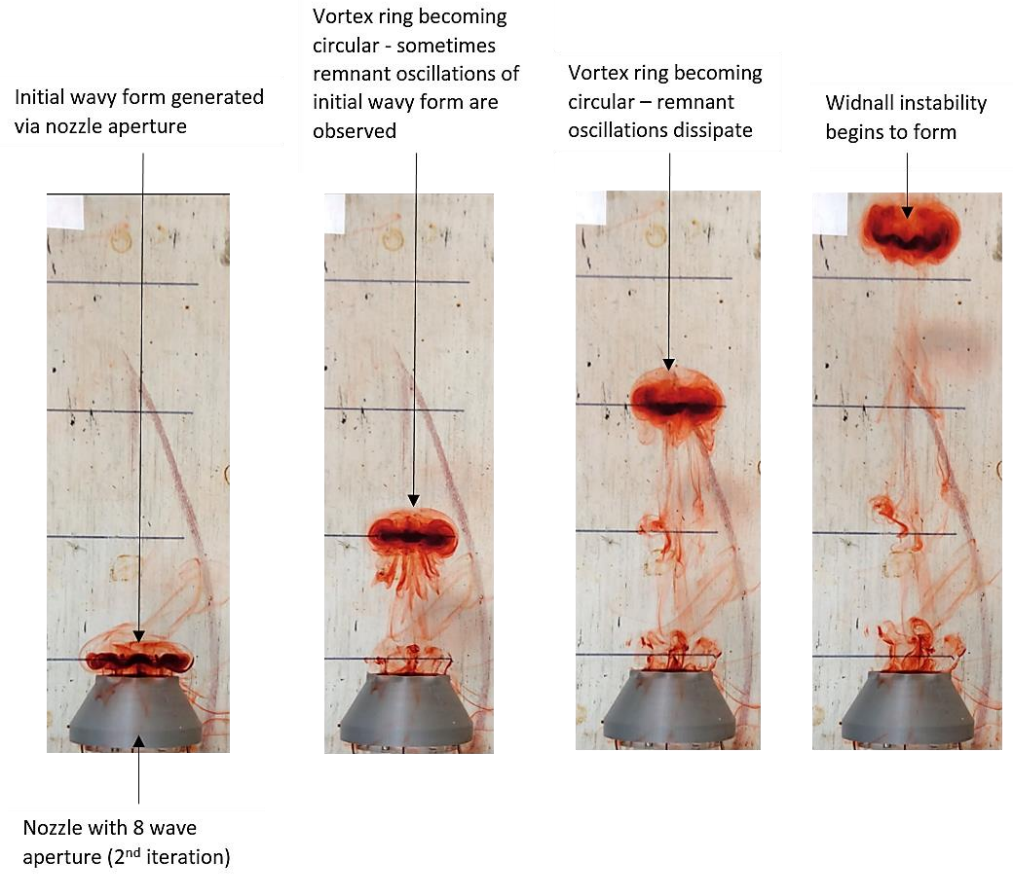

Figure 44 - Plan view of instability produced via 8 wave nozzle – Wavy shape; Flat; Flat; Instability

It was observed that the mode of the Widnall instability was not identical to the aperture of the nozzle, and instead, was still the mode as previously recorded based on the generation parameters. An example of this is shown in Figure 45, where although the shape of the nozzle and therefore the initial shape of the vortex ring resembled an 8 wave instability, the vortex ring eventually transitioned into the expected 7 wave instability before decaying.

It was observed, that although the initially shaped ring often returned to a circular form, it was rarely perfectly laminar and often showed additional turbulences as well as not remaining perfectly circular. Rather than perfectly circular, some of the clearest recordings indicate the majority of the vortex rings to show some small oscillations within the core of the ring before eventually forming the instability (cf. Figure 45 C and D).

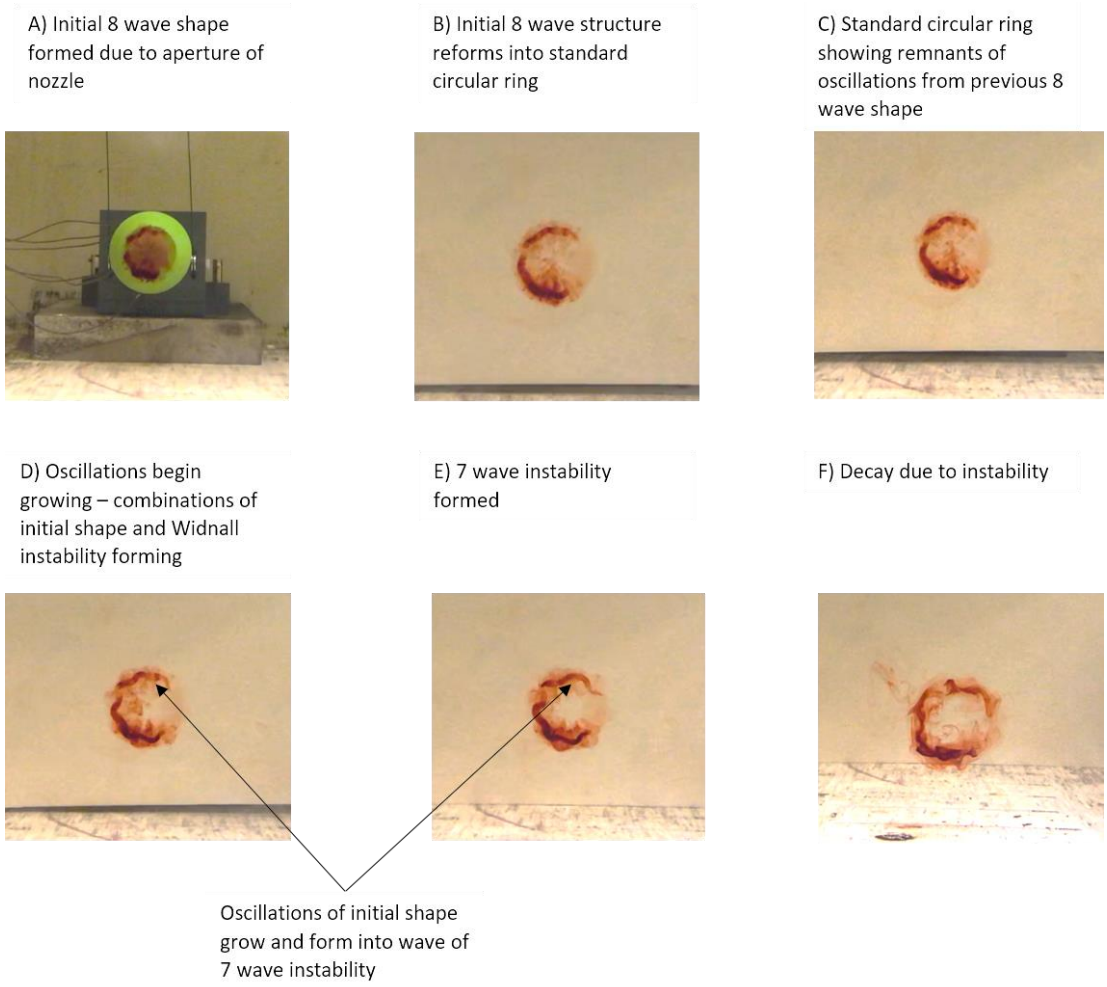

Figure 45 - Gradual Transition from 8 wave shape to 7 wave instability (wavy nozzle loaded with 75g)

As noted in Figure 45, sometimes it was observed that the oscillations of the initially formed shape grew and joined to form a wave of the instability. This was more often observed for scenarios where the imposed shaped was a similar mode to the naturally generated instability.

6 ANALYSIS

6.1 TRANSLATIONAL VELOCITY

6.1.1 Experimental Comparison

The recorded data approximately followed an e function as previously noted by researchers. The translational velocity of the data recorded, was compared with Krutzsch's data based on similar Reynold's numbers and instability modes.

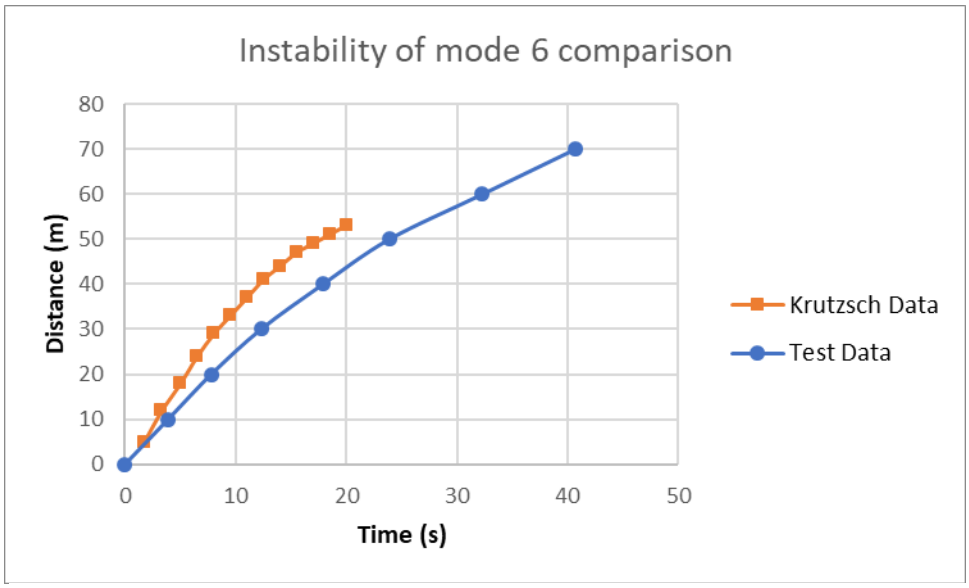

Figure 46 - Comparison between Nr. 14 and Nr. 1 Table 2

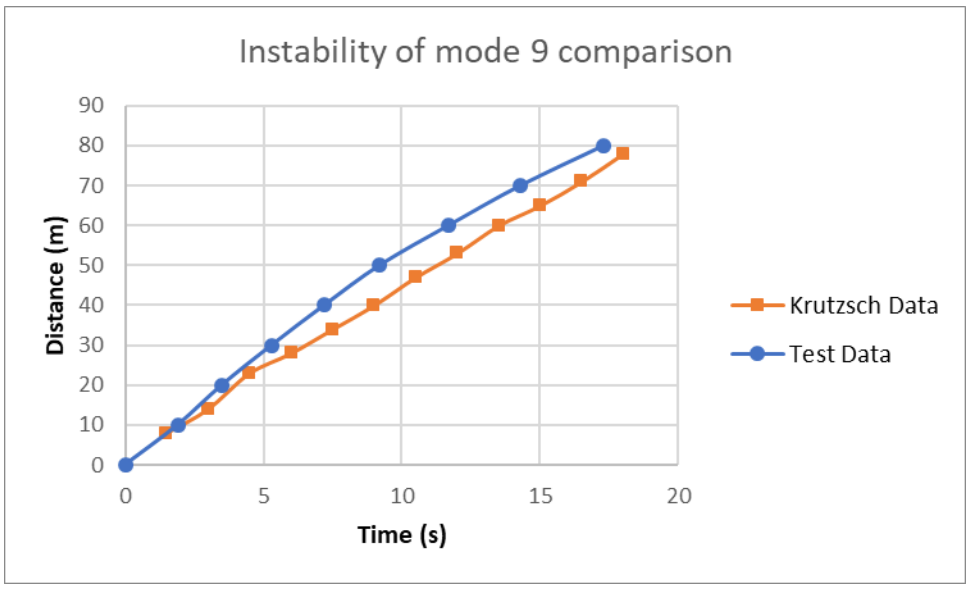

Figure 47 - Comparison between Nr. 5 Table 1 and Nr. 4 Table 2

A likely cause of the disparity between the two sets of data is the difference in the nozzle sizes for each experimental procedure. Krutzsch (Krutzsch, 1939) used two nozzles, one of 3cm and one of 7.6cm, whereas the experimental apparatus for this experiment used a nozzle of 5cm. This being a cause of the disparity is supported by the type of error shown in Figure 46 and Figure 47. In Figure 46 the data recorded by Krutzsch shows the rings velocity to be slightly greater. It is likely that this is due to the Krutzsch's nozzle being 3cm rather than 5cm, as Equation 2 implies that a smaller diameter produces a ring with a faster translational velocity. Figure 47 shows the opposite disparity, where the experimental data of the project is faster than Krutzsch's. This is due to this data being produced by a 5cm nozzle rather than a 7.6cm nozzle, again supported by Equation 2.

6.1.2 Theoretical comparison

The expected theoretical results for the translational velocity of the rings was calculated using Equation 1 and plotted against the experimental results for comparison.

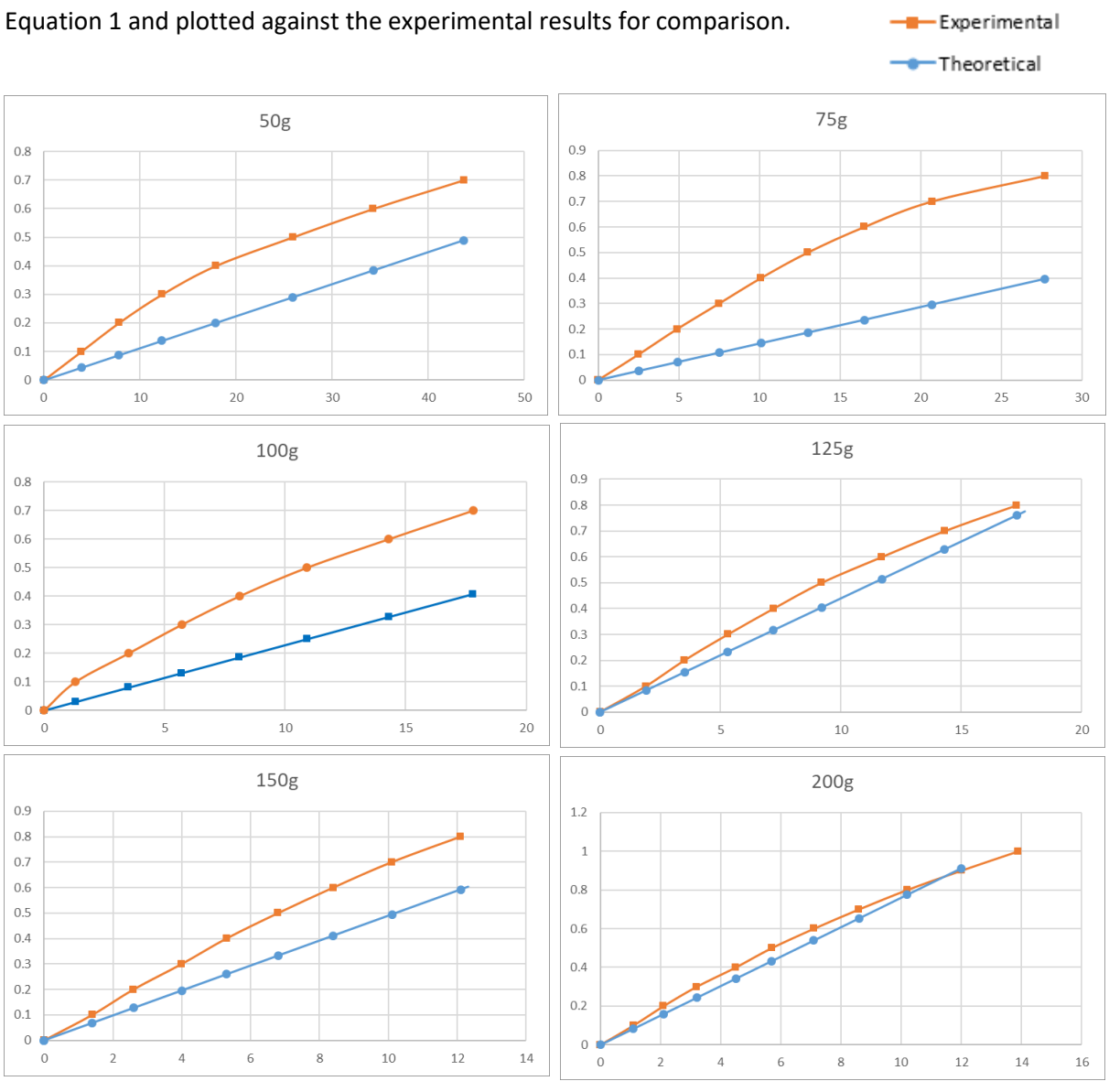

Figure 48 - Experimental Vs Theoretical Velocities

The difference between the theoretical and experimental results could be attributed to various factors. Potential factors could be fluctuations of the fluid, time was given in between each test run to allow for the water to steady, however, realistically unless it was left for a significant period of time, there would always have been fluctuations in the tank. It is unlikely that a systematic error could have caused the disparity, as errors such as the parallax error for the recording of the data were gauged and deemed relatively small. Rather than an experimental error, it is more likely that the error lies within the theoretical prediction. This is likely as the circulation, ring diameter and core radius were all estimations. The circulation was based off the slug approximation which used an average velocity of the piston. The ring diameter and core radius both had an error associated with measuring them as the method of measuring relied on estimating where the core radius seemed approximately equal and clearly defined.

6.1.3 The circular nozzle Vs The wavy nozzle

The vortex rings produced by the wavy nozzle were consistently slightly slower than the vortex rings produced by the circular nozzle (Figure 34. This could possibly be due to the vortex rings produced by the wavy nozzle being more turbulent. Even though the second iteration of the nozzle mitigated some of the added turbulence induced in the ring, there was still significantly more turbulence present in the rings generated by the wavy nozzle than the circular nozzle. The energy of the vortex ring being partially used in turbulence, rather than entirely on forward propagation like the circular nozzle, would have an adverse effect on the velocity of the ring. In addition to this, turbulence increases the rate of entrainment and therefore, the rate of volume increase of the vortex ring, this would induce a greater deceleration of the vortex ring, as supported by the majority of the figures. The volume of the ring was not noticeably larger and therefore it is reasonable to assume that the velocity decrease is most likely more affected by the direct loss of energy to turbulence. As the loaded weight is increased, so is the velocity of the piston and therefore the Reynolds number of the ring. This produced a more turbulent ring which in turn had a greater adverse effect on the velocity of the ring, as shown by the increasing disparity between the data as the loaded weight is increased.

6.2 INSTABILITY FORMATION

The experimental results were compared with various previous research. Comparing Table 5 – Circular Nozzle Instability Data with Table 1- Krutzsch's data (Krutzsch, 1939) shows a clear correlation. For example, Krutzsch's data for an instability with a mode of 7 forms at an Re_r of around 2050 for a 3cm nozzle and around 3800 for a 7.6cm nozzle. Therefore, the Reynolds number of the experimental data using a 5cm nozzle was expected to fall within this range, Table 2 shows it to be 2220. In addition to this, examples such as an instability with a mode of 9 for Krutzsch's data has a Re_r of 3770 (7.2cm nozzle), while the experimental data produced the same instability at a Re_r of 3270. The Reynolds number being slightly smaller was expected due to the slightly smaller nozzle size.

In addition to the comparable Reynolds numbers, the distance before becoming turbulent due to the instability also falls within the expected range. Comparing the tables, for a 3cm nozzle, the distances range between 20 and 40cm while the 7.6cm nozzle's vortex ring became turbulent between 70 and 100cm. Therefore, the range of the 5cm nozzle's data varying between 30 and 70cm is plausible.

Further comparison between more recent research, for instance Figure 8 from (Saffman, 1977) also shows promising results. The data was superposed onto the plot displaying the dependence of the mode on the Reynolds number. The data points from the experiment were plotted in orange, while Saffman's data was plotted in blue (cf. Figure 49). The data points correspond well to the proposed logarithmic trend line of Saffman.

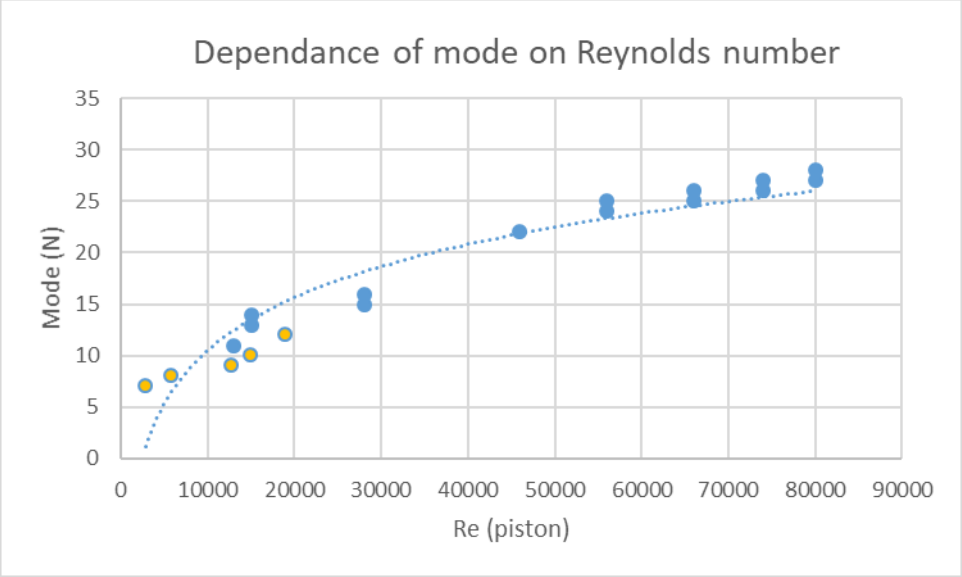

Figure 49 - Dependence of mode on Reynolds number. Experimental data was marked as orange, Saffman's data was marked as Blue.

6.3 IMPOSING AN INSTABILITY

6.3.1 The imposed shape

Observing the shape imposed by the wavy nozzles, it became clear that this was not an instability.

The propagation of the initial wavy shape is shown below.

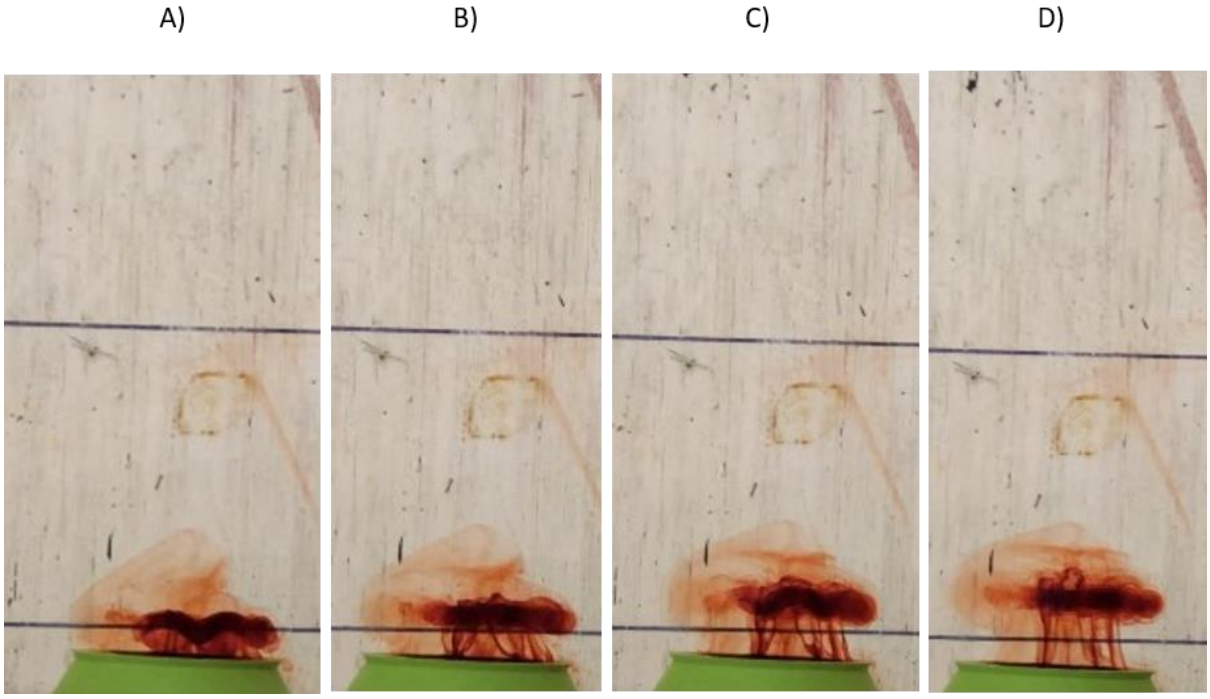

Figure 50 - Propagation of imposed wavy form – A) B) C) D)

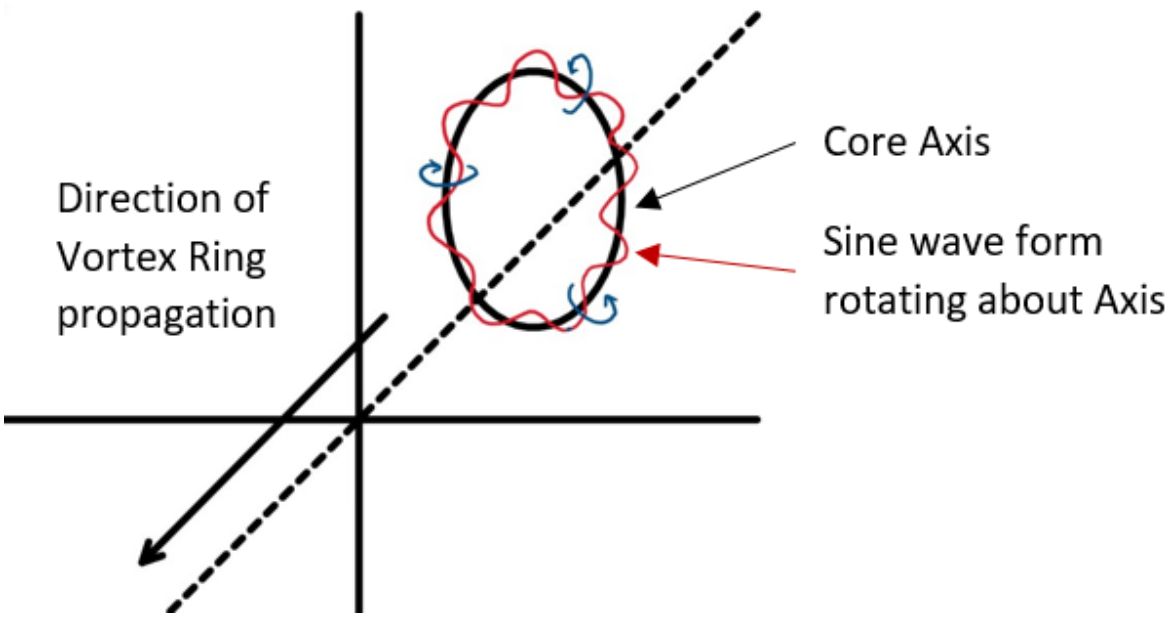

Figure 51 - Diagram to illustrate motion of imposed wavy form

As shown in Figure 51, the wavy form is a series of sin waves rotating about the core axis.

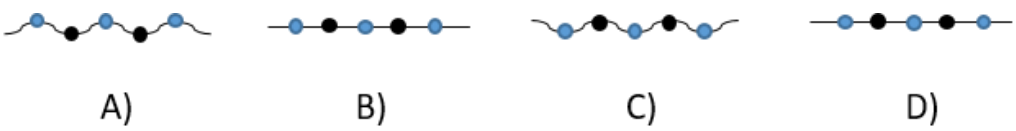

Figure 52 – Top-Down view of shape propagation. Diagram of Figure 50

As the form rotates, the peaks and troughs of A) become parallel to the top-down view making the form look straight as shown in B). The rotation of the wave from A) to C) appears as if the troughs have become peaks however this is the form rotating 180° about the axis of the core.

The wavy shape of an instability does not rotate about the axis but instead amplifies outwards (cf. Figure 39). As this is not how the imposed form propagates, it is clear that although the wavy form has a similar shape to an instability, it is produced, moves and functions in an entirely different way.

It is likely that the reason this aperture did not produce an instability, was that the core concept of stability theory regarding an instability and its amplification is that it starts via a very small disturbance. The large protrusions of the wavy nozzle were not a small disturbance relative to the system and therefore produces a completely different flow. These protrusions do however displace the roll up of the vortex sheet in the same shape and therefore produce a vortex core following this shape.

6.3.2 Variation between the nozzles

Although the 2nd iteration of the wavy nozzle theoretically was expected to perform better in the production of wavy rings, some of the clearest data displaying the second scenario was produced via the first iteration of nozzle.

While searching for a possible explanation, it was proposed that the small lip causing turbulence possibly helped preserve the shape. With a perfectly smooth transition into the aperture (2nd iteration), it is possible that this perfectly laminar flow, once contorted into the specific wavy shape of the aperture quickly became significantly turbulent. This would produce the first scenario where the fluid retains the shape for a short distance before quickly becoming turbulent and then dissipating. A lip as a minor protrusion to the boundary layer, however, could instigate minor turbulence that would facilitate the passing through the aperture in a more stable form without instantly becoming extremely turbulent. It is feasible that once this shape begins transitioning back to a circular shape, the turbulence has diffused and the ring is once again relatively laminar facilitating the transition back to turbulence via the standard instability.

6.3.3 Observation – When shape mode is similar to instability mode

As observed in Figure 45, two of the remnant oscillations from the initially formed shape appeared to grow slightly before forming into one wave of the natural instability. From this, although it is still observed in general that the imposed shape and resultant instability are independent, it may be the case that the imposed shape could have some alternative effect on the formation process of the instability.

7 CONCLUSION

The experiment successfully produced and recorded vortex rings generated under various different parameters. The properties of the translation and Widnall instability were compared with previous research and showed considerable correlation, supporting that the recorded data is valid.

In addition to studying previously researched data, the theory of potentially imposing an instability was also explored. The attempt to impose an instability was unsuccessful as although it had a similar shape to an instability, it was clearly not an actual instability due to the way it moved. It did however provide an interesting conclusion to imposing a complex shape on a vortex ring, displaying the shape formation, returning to a standard laminar ring before then beginning the process of forming a natural instability.

This did not disprove the possibility of imposing an instability on a vortex ring, and future projects considering this research should possibly explore the effect of much smaller protrusions on the aperture to see whether this correlates better with the theory of initiating the Widnall instability.

8 REFERENCES

Adhikari, D., 2009. *SOME EXPERIMENTAL STUDIES ON VORTEX RING,* Singapore: NATIONAL UNIVERSITY OF SINGAPORE.

Aitchtuoh, F., 2015. *Central Florida Aquarium Society.* [Online]
Available at: https://cflas.org/2015/08/31/dolphin-plays-with-toroidal-vortex/
[Accessed 18 February 2020].

Akhmetov, D., 2009. *Vortex Rings.* 1st ed. Berlin: Springer.

Akhmetov, D. G., Lugovtsov, B. A. & Tarasov, V. F., 1980. Extinguishing gas and oil well fires by means of vortex rings. *Fiz. Goreniya Vzryva,* Volume 5, pp. 8-14.

Akhmetov, D. L. B. A. T. V. F., 1980. EXTINGUISHING GAS AND OIL WELL FIRES BY MEANS OF VORTEX RINGS. *COMBUSTION EXPLOSION AND SHOCK WAVES,* 16(5), pp. 490-494.

Burk, S., 2011. *Experiments Involving Vortex Rings,* Coventry: University of Warwick.

Costello, J. H., Colin, S. P., Gemmell, B. J. & Dabiri, J. O., 2019. Hydrodynamics of Vortex Generation during Bell Contraction by the Hydromedusa Eutonina indicans. *BIOMIMETICS,* 4(3).

Crow, S. C., 1970. Stability theory for a pair of trailing vortices. *American Institute of Aeronautics and Astronautics,* 8(12), pp. 2172-2179.

De Bernardinis & Dhanak, 1981. THE EVOLUTION OF AN ELLIPTIC VORTEX RING. *JOURNAL OF FLUID MECHANICS,* 109(8), pp. 189-216.

Didden, N., 1979. On the Formation of Vortex Rings: Rolling-up and Production of Circulation. *ZEITSCHRIFT FUR ANGEWANDTE MATHEMATIK UND PHYSIK,* 30(1), pp. 101-116.

Glezer, A., 1988. The formation of vortex rings. *The Physics of Fluids,* 31(12), pp. 3532-3542.

Gorder, P. F., 2004. Vortex Drive. *NewScientist,* 184(2470), pp. 31-34.

Helmholtz, H., 1858. Ueber Integrale der hydrodynamischen Gleichungen, welche den Wirbelbewegungen entsprechen. *J. Reine Angew. Math,* 55(1), pp. 25-55.

Hicks, W. M., 1885. XV. Researches on the theory of vortex rings.—Part II. *Philosophical Transactions of the Royal Society of London,* pp. 725-780.

Huang, J. & Chan, K. T., 2007. *Dual-Wavelike Instability in Vortex Rings.* Athens, 5th IASME / WSEAS International Conference on Fluid Mechanics and Aerodynamics August 25-27, , pp. 258-262.

Huang, J. C. K., 2007. *Dual-Wavelike Instability in Vortex Rings.* Athens, s.n.

Krueger, P., 2005. An over-pressure correction to the slug model for vortex ring circulation. *JOURNAL OF FLUID MECHANICS,* Volume 545, pp. 427-443.

Krutzsch, C. H., 1939. Über eine experimentell beobachtete Erscheinung an Wirbelringen bei ihrer translatorischen Bewegung in wirklichen Flüssigkeiten. *Annalen der Physik,* 427(6), pp. 497-523.

Kuchemann, 1965. *J. fluid Mech,* Volume 21.

Lundgren, T. & Mansour, N., 1991. VORTEX RING BUBBLES. *Journal of Fluid Mechanics,* Volume 224, pp. 177-196.

Mansi, C., 2019. *Experimental study on vortex rings in air (exact title of thesis unknown),* Coventry: University of Warwick.

Maxworthy, T., 1972. The structure and stability of vortex rings. *J. Fluid Mech.,* 51(1), pp. 15-32.

Maxworthy, T., 1977. Some experimental studies of vortex rings. *J. Fluid Mech.,* 81(3), pp. 465-495.

Pinheiro, M. J., 2014. *The Soul of Matter.* [Online]
Available at: https://soulofmatter.wordpress.com/2014/03/02/nuclear-explosion-and-vortex-ring/comment-page-1/
[Accessed 18 February 2020].

RapidTables, 2016. *Online Ruler.* [Online]
Available at: https://www.rapidtables.com/web/tools/pixel-ruler.html
[Accessed 4 3 2020].

Reynolds, O., 1876. On the Resistance Encountered by Vortex Rings and the Relation between Vortex Rings and the Stream-Lines of a Disc.. *Nature,* 477(14).

Reynolds, O., 1883. An Experimental Investigation of the Circumstances Which Determine Whether the Motion of Water Shall Be Direct or Sinuous, and of the Law of Resistance in Parallel Channels. [Abstract]. *Proceedings of the Royal Society of London,* Volume 35, pp. 84-99.

Saffman, P. G., 1970. VELOCITY OF VISCOUS VORTEX RINGS. *STUDIES IN APPLIED MATHEMATICS,* 49(4), pp. 371-&.

Saffman, P. G., 1977. The number of waves on unstable vortex rings. *Journal of Fluid Mechanics,* 84(4), pp. 625-639.

Saffman, P. G., 1995. *Vortex Dynamics.* 1st ed. Cambridge: Cambridge University Press.

Thompson, P. S. W., 1867. On vortex atoms. *Phil. Mag.,* Volume 34, pp. 15-24.

White, F. M., 2008. *Fluid Mechanics.* 6th ed. New York: McGraw-Hill.

Widnall, S. E., 1971. *THEORETICAL AND EXPERIMENTAL STUDY OF THE STABILITY OF A VORTEX PAIR,* Boston: Springer.

Widnall, S. E., 1975. THE STRUCTURE AND DYNAMICS OF VORTEX FILAMENTS. *ANNUAL REVIEW OF FLUID MECHANICS,* Volume 7, pp. 141-165.

Widnall, S. E. a. J. P. S., 1973. On the Stability of Vortex Rings. *Mathematical and Physical Sciences,* Volume 332, pp. 335-353.

Widnall, S. E., Bliss, D. B. & Tsai, C.-Y., 1974. The instability of short waves on a vortex ring. *J. Fluid Mech.,* Volume 66, pp. 35-47.

Wolf, M., 2013. Structure of the vortex wake in hovering Anna's hummingbirds (Calypte anna). *PROCEEDINGS OF THE ROYAL SOCIETY B-BIOLOGICAL SCIENCES,* 280(1773).